ABSTRACT

GUJARATI, AKASH MAYUR. Performance and Control of a Hybrid Active Filter Enabled Interface of a HVDC Converter Station for Weak AC Systems. (Under the direction of Dr. Subhashish Bhattacharya).

The high voltage direct current (HVDC) converter is a nonlinear load that injects harmonic currents back into the AC network that it is connected to. Harmonic distortion is, thus, a major issue for HVDC converter stations since it can adversely affect the voltage quality and cause malfunctioning of the equipment and loads that are connected to the AC grid. Hybrid active filters (HAF) are able to overcome the resonance and detuning issues of passive filters as well as the rating problems of pure active filters.

A HAF topology is proposed in this thesis that combines a damped double tuned passive filter with an active filter. The passive filter is tuned to remove the dominant harmonics and also the higher frequency currents while also providing reactive power support to the HVDC converter. The active filter is connected to the passive filter in a way that ensures minimal fundamental voltage across it and also that the fundamental current is diverted away from it through the passive branch, thereby reducing the active filter rating. The control of the active filter is done using a proportional-resonant regulator in the synchronous reference frame. This method allows the compensation of the positive sequence and negative sequence dominant harmonics using a single controller.

The operation of the proposed HAF with the proportional-resonant controller is verified using time domain simulations in PSCAD. The results show that the HAF is effective in filtering the harmonic currents even during system resonance conditions that cause the passive filters to be ineffective.

Performance and Control of a Hybrid Active Filter Enabled Interface of HVDC Converter Station for Weak AC Systems

by
Akash M. Gujarati

A thesis submitted to the Graduate Faculty of
North Carolina State University
in partial fulfillment of the
requirements for the degree of
Master of Science

Electrical Engineering

Raleigh, North Carolina

2014

APPROVED BY:

_____
Dr. Subhashish Bhattacharya
Chair of Advisory Committee

_____ _____
Dr. Jayant Baliga Dr. Mesut Baran

BIOGRAPHY

Akash Gujarati is from Pune, India and came to NC State University as a student-athlete to play for the Division I tennis team. He received his Bachelor of Science degree in Electrical Engineering with honors from NC State University in 2012 and continued on for his graduate studies.

ACKNOWLEDGMENTS

I would like to thank my family for their support and contributions.

Also, I want to add an expression of gratitude to everyone else that made it possible for me to achieve this degree.

TABLE OF CONTENTS

LIST OF TABLES

LIST OF FIGURES

CHAPTER 1

Introduction

In the last few decades, HVDC power transmission has become an economically feasible and competitive alternative to the conventional high voltage alternating current (AC) transmission for a number of applications. One of the main advantages of AC transmission is the ability to step-up and step-down the voltage with a transformer that has a very high efficiency. The use of converters to transform voltage from AC-DC and vice versa was limited to low voltage applications, many years ago, but the improvement in semiconductor technology has spurred the usage of HVDC. In spite of the high cost of the HVDC converter, this method of transmission is less expensive for transferring bulk power over long distances due to the lower cost of the transmission system. Moreover, HVDC is required to connect asynchronous networks, utilize long underground cables or subsea cables for offshore power transmission, share utility rights-of-way without degradation of reliability, and some other applications. With the advances in semiconductor technology, it is possible to operate these converters at very high voltage and current ratings.

The traditional HVDC converter is thyristor based where the switch is commutated directly by the line and is, therefore, called a line commutated converter. Thyristors can be fabricated to block extremely high voltages and they are also considerably inexpensive which makes the LCC technology a very good choice for maximum bulk power transfer. However, LCC HVDC has a few disadvantages such as being susceptible to commutation failure in

inverter mode of operation, the consumption of significant amount of reactive power, and the injection of harmonics into the commutating network. This further necessitates a strong grid with a high short circuit ratio and the employment of capacitor banks and harmonic filters. A relatively recent solution to some of these problems is the use of insulated gate bipolar transistor (IGBT) switched voltage source converters. The IGBT does not rely on negative voltage to stop conducting current through it and can be turned off by supplying the appropriate gate signal. This gives the IGBT based converters full control over the phase of the current with respect to the voltage and in turn allows the converter to regulate the active and reactive power flow. The VSC can function even when connected to a weak grid since it doesn't depend on the line voltage for commutation. However, these switches are not able to match the high voltage capability of the cheaper thyristors and hence, can only be used for relatively lower power ratings. Hence, the HVDC converter is usually associated with the thyristor switched converter, which as stated before, has the problem of harmonic current injection into the grid. This provides the motivation for the development of methods to filter the harmonic currents that are created by the converter in a HVDC system.

CHAPTER 2 goes into detail about the problem of harmonic distortion due to HVDC converters and briefly summarizes the standards to measure the harmonic performance of a HVDC converter station. The issues of system resonance and detuning of the passive filters which make the solution presented in this thesis necessary are also discussed.

CHAPTER 3 looks at the considerations to design a HVDC system including the LCC, transformer, and passive filters. The analysis of the LCC from [1] is used to design the parameters for the converter. The designed system is tested with grid values that cause system resonance and the results are documented. This is followed by a discussion of active filters in CHAPTER 4 and also a short passage about the failings of pure active filters for HVDC. In CHAPTER 5 the HAF is reviewed as a solution and a unique HAF topology is proposed based on the configuration in [2]. The controls for the proposed HAF are also developed and tested. The results of the time domain simulations of the HVDC system with the proposed HAF are reported in CHAPTER 6 and finally, the summary and scope of the work done is presented in CHAPTER 7.

The appendix provides information about the synchronous reference frame (SRF) transformation convention used. Additional results from time domain simulations using another simulation tool (PLECS) are also documented in the appendix.

CHAPTER 2

Harmonic Distortion

2.1 Background

There are many nonlinear loads connected to the AC network that include static power converters, arc discharge devices, saturated magnetic devices, and rotating machines The power converters are the largest nonlinear loads and are used for many purposes because they can convert AC signals to DC and vice versa. However, these loads change the sinusoidal waveform of the AC network and introduce the flow of harmonic currents that can cause various problems. They can also result in high levels of harmonic voltage due to the use of capacitors on the line. Thus, it is important to quantify the harmonic distortion of the power system and take steps to avoid its occurrence.

2.2 Harmonic Generation

Harmonic distortion is created due to the nonlinear characteristics of the devices and loads in the power system. The device is nonlinear when the relationship between the instantaneous voltage and current is not linear. The HVDC converter has a nonlinear current and voltage waveform for the synthesis of the three phase line voltages into a DC voltage, and is thus, a source of harmonic currents which are injected back into the ac grid network. The magnitude and frequency of the generated currents can be mathematically solved for an ideal case by creating a model for the converter. An ideal model is considered with no

commutation angle and the ac voltage is taken to be balanced and the dc current constant in the derivation of the equation for the converter current that follows.

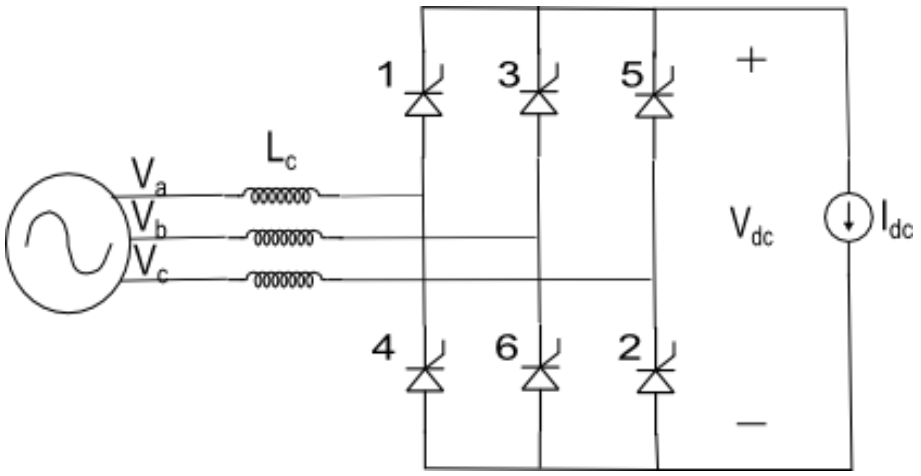

Figure 2.1: A 6-pulse HVDC converter

The thyristors in the Figure 2.1 are numbered according to the order in which they conduct, where at any given moment there are two thyristors conducting. For instance, when the line voltage, V_{ac}, is positive then switches 1 and 2 conduct the DC current. This is followed by commutation of the current from switch 1 to switch 3, and so on. The phase voltage and current waveforms are seen in Figure 2.2.

The Fourier analysis of the phase currents can be done to obtain an equation that describes the line current,

$$I_{s,WYE} = \frac{2\sqrt{3}}{\pi} I_{dc} \left[\cos \omega t - \frac{1}{5}\cos 5\omega t + \frac{1}{7}\cos 7\omega t \right.$$

$$\left. - \frac{1}{11}\cos 11\omega t + \frac{1}{13}\cos 13\omega t - \cdots \right] \quad (1)$$

The magnitude of the harmonics of the fundamental are scaled by a factor of 1/n where n is the harmonic number. This is the ideal case for a wye connected converter.

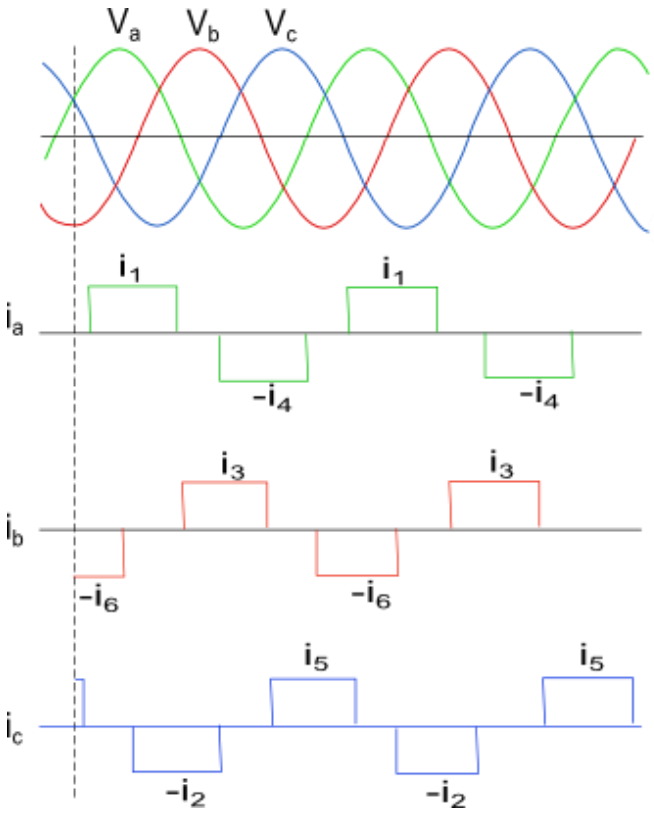

Figure 2.2: LCC voltage and current waveforms.

The current for a delta connected converter is described by a slightly different equation where the signs of the harmonic terms change due to the phase lag/lead of the delta connected converter voltage with respect to the primary voltage.

$$I_{s,DEL} = \frac{2\sqrt{3}}{\pi} I_{dc} \left[\cos \omega t + \frac{1}{5}\cos 5\omega t - \frac{1}{7}\cos 7\omega t - \frac{1}{11}\cos 11\omega t + \frac{1}{13}\cos 13\omega t - \cdots\right] \quad (2)$$

The observed harmonic current magnitude of a HVDC converter for a practical case is generally lower because of the impedance presented by the commutating reactance of the line. The detailed operation of the LCC will be investigated in Chapter 3.

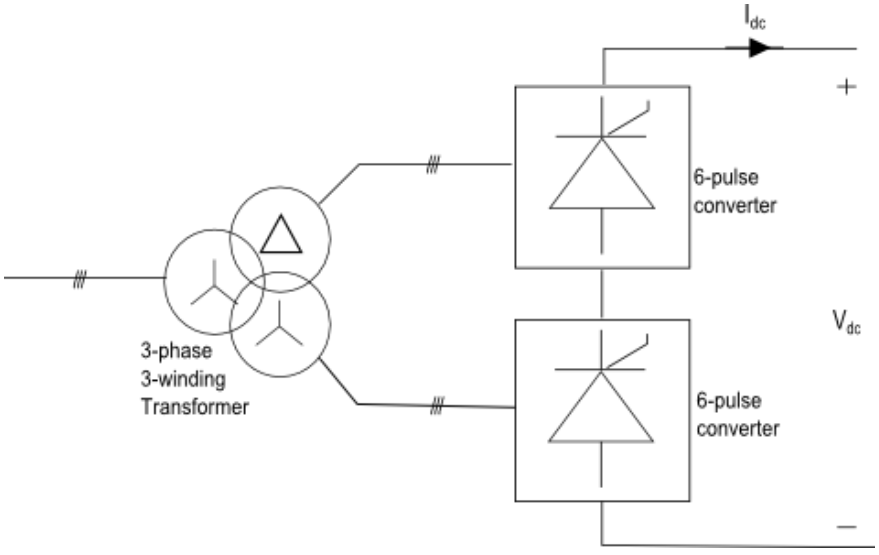

Figure 2.3: 12-pulse HVDC converter

The modern HVDC station has a 12-pulse converter which consists of two 6-pulse converters, one connected to a Y-Y converter transformer and the other connected to a Y-Δ transformer. As is seen from (1) and (2) the signs of some of the harmonic terms of the wye connected converter are the opposite of the delta connected converter. Thus some of the harmonics are cancelled out by using a 12 pulse converter with careful design of the transformer reactance and synchronized firing pulse generation.

$$I_{s,primary} = \frac{2\sqrt{3}}{\pi} I_{dc} \left[\cos \omega t - \frac{1}{11}\cos 11\omega t + \frac{1}{13}\cos 13\omega t - \frac{1}{23}\cos 23\omega t + \frac{1}{25}\cos 25\omega t - \cdots\right] \quad (3)$$

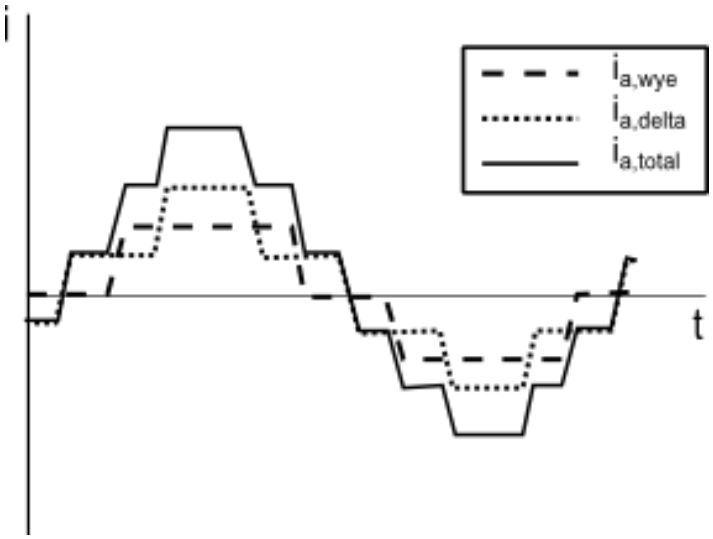

Figure 2.4: 12-pulse converter current waveform

In short, for a n-pulse converter the order of harmonics, h, that is introduced into the AC system is

$$h = kn \pm 1 \qquad (4)$$

$$where\ k\ is\ a\ positive\ integer$$

Thus, the lower order harmonics can be eliminated by using higher pulse converters. However, HVDC power transmission studies have shown that pulse numbers higher than 12 are not economical due to added complexities of the system [3].

A small magnitude of non-characteristic harmonics can also be introduced into the network due to firing angle errors and unbalances in the converter transformer reactance and the supply voltage. The phase mismatch on the AC side can generate odd harmonics while the firing angle error of the converters can also create even harmonics. These harmonics are usually neglected in harmonic studies since they have very low values.

Any nonlinear device such as a generator or power transformer will create harmonics in the ac network. Loads on the distribution network also add to the harmonic content of the grid. For this reason, the grid cannot be considered to be ideal when designing harmonic filters for converter stations.

2.3 Effects of Harmonic Distortion

The presence of harmonics in the grid network can cause serious problems and adversely affect the quality of the voltage. Some ill-effects of harmonics are listed here –

a. **Interference with telephone lines** – It is common practice for telephone lines to utilize the same infrastructure as transmission lines. If there are harmonics in the ac network these can interact with the adjacent communication lines and cause interference.

b. **Over-loading of capacitors** – Fixed capacitors are used to improve the voltage profile of the line and also provide reactive power to the HVDC converter. If there is any resonance with the converter system at a higher frequency then the amount of harmonic current into the capacitor can amplify and cause over-loading. Even without overloading, the harmonic currents can increase the stress on the capacitor and result in a shortened capacitor life.

c. **Equipment malfunction** – In a similar way that the harmonics harm capacitors, other grid connected equipment can also be harmed due to increased heating. All rotating machinery heat up due to iron and copper losses at harmonic frequencies reducing the efficiency and also the torque produced. Similarly, copper losses and stray flux losses result due to harmonic currents in transformers.

d. **Metering errors** – It is possible for harmonics to cause inaccurate measurements of currents, voltages and power. Mainly, during resonant conditions the amplified harmonic voltage and current values can cause a reduced power factor which is not differentiated by the measuring devices resulting in incorrect meter readings. [4]

2.4 Harmonic Filters

It is apparent from the previous section that harmonic distortion in the AC network is very harmful and has to be eliminated. One way of filtering the harmonics is providing the high frequency currents a low impedance path using the combination of capacitors, inductors and resistors. These types of filters are called passive filters since they are comprised of passive elements. In addition to sinking the harmonic currents, these can also be used to provide reactive power support to the HVDC converter. A variety of filters can be employed specific to the need of filtering at the particular converter station. A short review of a few basic filters is presented in this section.

2.4.1 Single tuned filter

A single tuned or band pass filter is the most basic passive filter topology which consists of a reactor connected to a capacitor bank. A resistor may be added in series (usually it is just the loss of the inductor) to provide damping at the tuned frequency and lower the quality factor. In designing a single tuned filter, the value of the capacitance, C, is chosen depending on the amount of reactive power support expected. The inductance, L, can then be chosen so that the impedance of the branch is tuned to a minimum at the desired frequency using the equation

$$\omega_n = \frac{1}{\sqrt{LC}} \qquad (5)$$

$$\omega_n = 2\pi f_0 n \quad (6)$$

$$where\ f_0 is\ the\ fundamental\ frequency\ and\ n\ is\ the\ harmonic\ number$$

If a certain quality factor, Q, is desired then the resistance, R, value can be chosen

$$Q = \frac{\omega_n L}{R} \quad (7)$$

so that the filter bandwidth increases and its performance around the tuned frequency is improved.

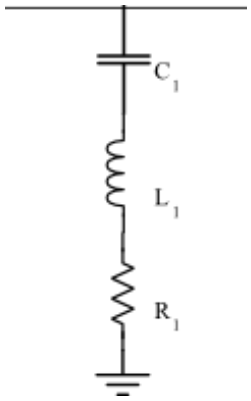

Figure 2.5: Single tuned or Band Pass Filter

However, this filter only provides attenuation for one harmonic so it is not able to provide filtering for changing grid and load conditions resulting in different orders of harmonics. Hence, multiple single tuned filter branches are needed. It is also susceptible to poor performance due to detuning.

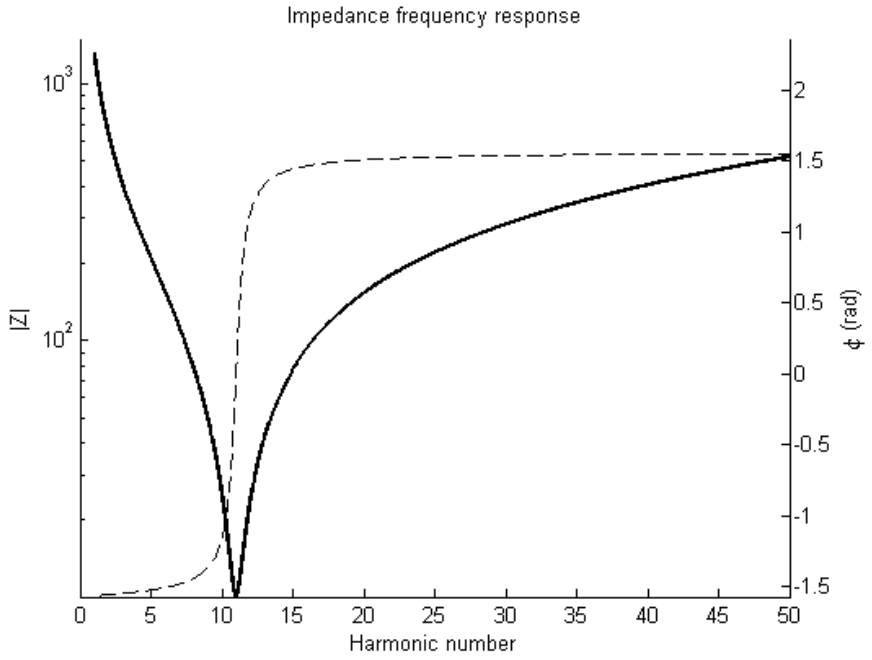

Figure 2.6: Bode plot of single tuned filter

2.4.2 Double tuned filter

This type of filter is the combination of two single tuned filters. The main advantage of a double tuned filter is that it provides filtering for two harmonics and requires only one high voltage capacitor and reactor. However, the rating of this capacitor is considerably higher if it is providing the same reactive power as the capacitors of the set of single tuned filters that it replaces.

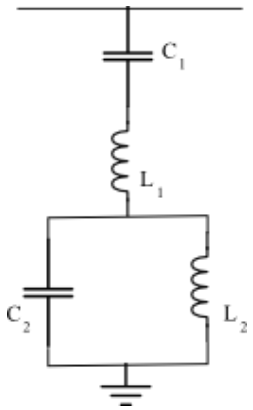

Figure 2.7: Double tuned filter

The performance of a double tuned filter can also suffer due to detuning and the complexity of the connections is increased when compared to single tuned filters.

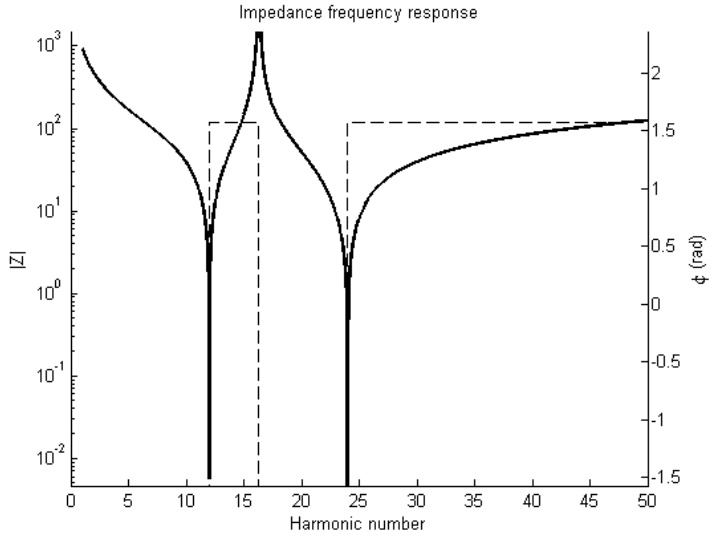

Figure 2.8: Bode plot of a double tuned filter

2.4.3 Damped double tuned filter

The double tuned filter can be modified to filter higher order harmonics and also improve the bandwidth at the tuned frequencies by using damping resistors. Two variations of damped double tuned filters are seen below with their impedance characteristics.

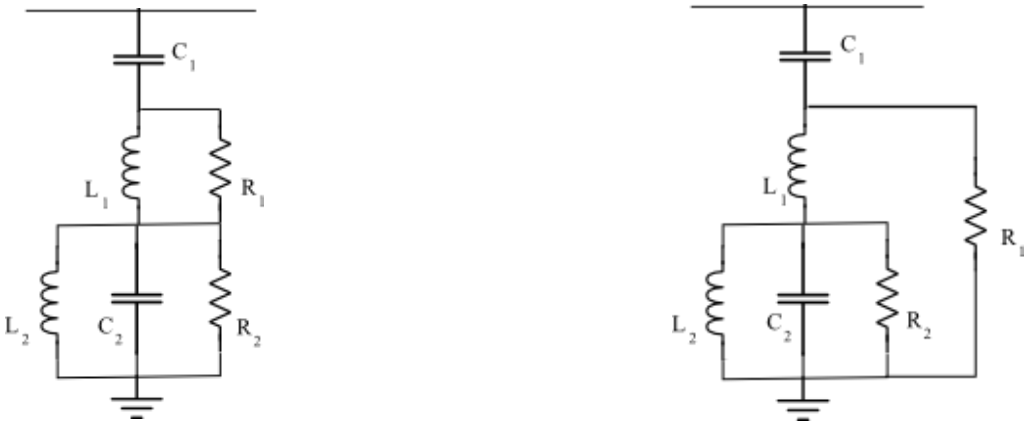

Type 1 **Type 2**

Figure 2.9: Damped double tuned filter

Damped double tuned filters offer a better frequency response and are less sensitive to detuning effects. However, the presence of damping resistors increases the power loss in these filters.

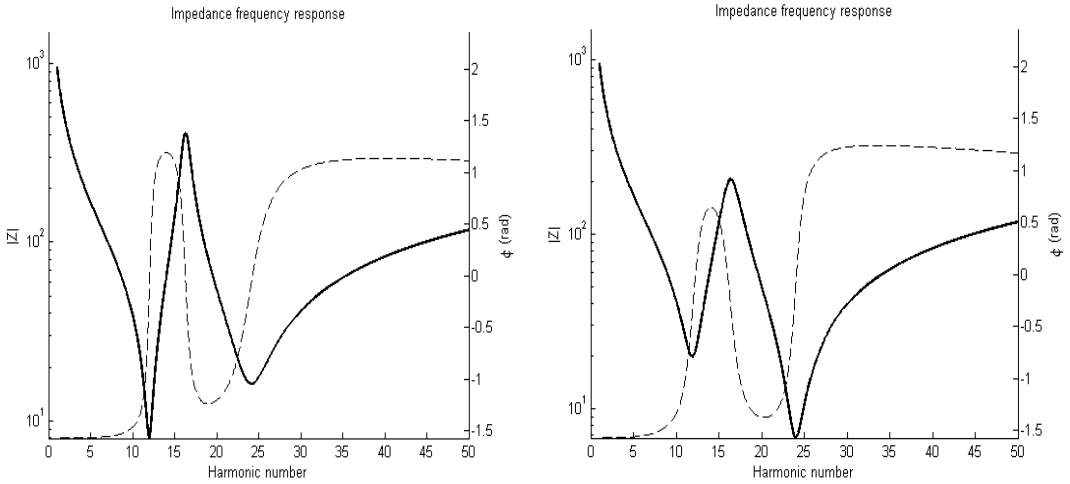

Type 1 **Type 2**

Figure 2.10: Bode plots of the damped double tuned filter

2.5 Harmonic Standards

The objective of the AC filter design is to limit the harmonic currents in the grid so as to meet certain standards put forth by the utility. The IEEE has its own harmonic performance specification that specifies the maximum allowable voltage and current distortion in the AC network at the HVDC converter station. These guidelines also vary with a particular project depending upon the customer needs. These include limits for harmonic voltage distortion and telephone interference. An overview of the commonly accepted performance guidelines is given below.

2.5.1 Voltage Distortion

The primary requirement for AC filters is to ensure that the AC network voltage quality is maintained and the distortion does not exceed the set limits. There are various

metrics to quantify the distortion in the grid among which the individual harmonic distortion (D) and the total harmonic distortion (THD) are most common among utilities. The individual harmonic distortion is a measure of the voltage content at the point of common coupling (PCC) of each harmonic frequency. For each harmonic, n, this is calculated by

$$D_n = \frac{V_n}{V_1} * 100\% \qquad (8)$$

where V_1 is the fundamental frequency line to neutral voltage (RMS).

The THD index corresponds to the power of the harmonics and is therefore more closely related to the severity of the disturbance in terms of heating effects [5]. The formula for computing the THD is

$$THD = \sqrt{\Sigma_{n=2}^{N} D_n^2} \qquad (9)$$

where the maximum frequency order, N, is generally set to 50 as the magnitude of the injected harmonics from the HVDC converter is sufficiently diminished at higher frequencies. Typically, the individual voltage distortion is to be kept under 1% and the THD is regulated between 1% and 4% depending on the system size.

2.5.2 Telephone Interference

The magnitude of the harmonic content in the AC network can be a source of interference in the communication lines. It is common for HVDC schemes to ensure compliance with the telephone interference limits. There are two criteria to measure

telephone interference at the PCC. The first one is a measure of the voltage telephone interference (VTIF) and the other is based on the harmonic currents (IT).

$$VTIF = \frac{\sqrt{\Sigma_{n=1}^{N}\left(V_n W_{fn}\right)^2}}{V_1} \qquad (10)$$

$$IT = \sqrt{\Sigma_{n=1}^{N}\left(I_n W_{fn}\right)^2} \qquad (11)$$

$$kIT = \frac{IT}{1000} \qquad (12)$$

where V_n and I_n are the harmonic voltage and current, and W_{fn} is the harmonic coupling factor.

However, these criteria vary greatly from utility to utility and depend on various factors. They are not extremely accurate in determining the effect of the harmonic distortion on the telephone lines. The coupling weighting is much larger for the higher frequency currents but at such high frequencies the current profile along the transmission lines is highly variable and is a complex function of the harmonic impedance of the network elements and configurations.

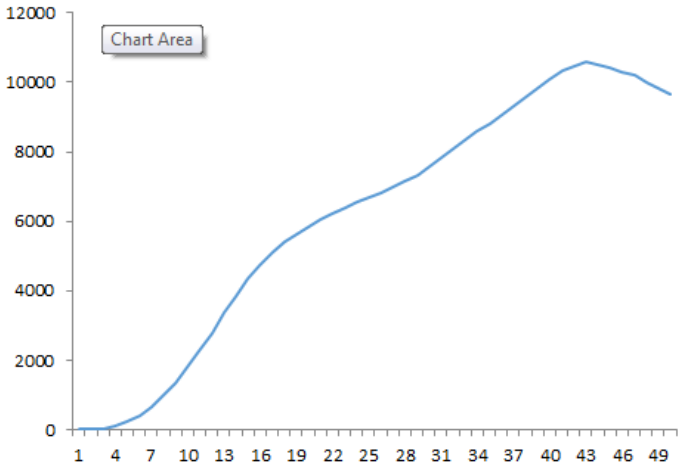

Figure 2.11: Psophometric weighting factor (W_{fn})

Some of the factors that are considered when defining the IT and VTIF boundaries are the density of telephone lines close to the ac network, the length and average separation from the AC lines, the type of the communication line and also the structure of the AC grid network. For the VTIF, the range between 25 and 50 is normally considered permissible while the kIT should be kept below 100 at the minimum.

The IEEE 519 Harmonic Standard for voltage distortion [6] is shown in Table 1.

Table 1: IEEE 519 Harmonic Standard for Voltage Distortion

Harmonic Voltage Distortion in % at PCC			
System voltage	2.3 – 69 kV	69 – 138 kV	>138 kV
D_n	3.0	1.5	1.0
THD	5.0	2.5	1.5

The current distortion standards vary as well depending on the short-circuit ratio (SCR) and can be looked up in [6].

2.6 Harmonic Performance Analysis

In order to meet the harmonic performance specifications stated in the previous section it is important to conduct a system study and analyze the interaction of the grid and the filters. This analysis can be done in the time domain using real time digital simulation techniques and also in the frequency domain by creating harmonic models for the entire system. A basic frequency domain analysis technique that serves as a good starting point is the single frequency study of the system where the HVDC converter is treated as a harmonic current source and the small signal analysis of the circuit comprising of the harmonic impedances of the grid and filters is done to calculate harmonic voltages and currents at the PCC. This method does not capture the harmonic interaction between the AC and the DC sides.

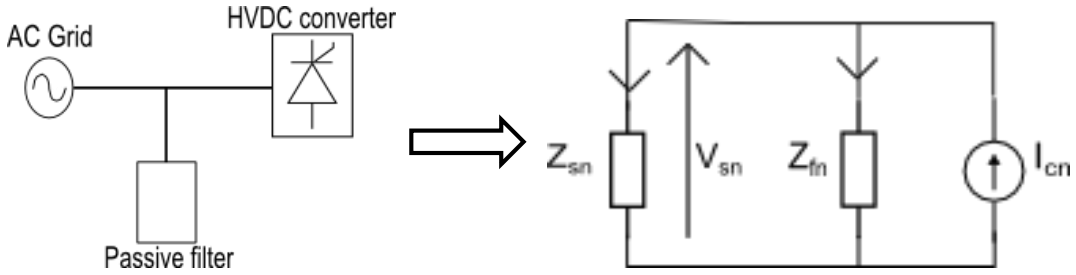

Figure 2.12: Representation of HVDC system for frequency domain analysis

Here, Z_{sn} is the system harmonic impedance and Z_{fn} is the filter harmonic impedance while the converter current is denoted by I_{cn}.

The time domain simulations can give more accurate data that can be recorded and analyzed in the frequency domain to measure the desired characteristics. In the time domain, the actual load flow analysis and the interaction in the power system is calculated in detail which makes the results more meaningful. However, a detailed model of the system is necessary to get good results. Software tools such as PSCAD are usually accepted for power system simulations.

2.6.1 System Impedance Modeling

A critical focus of AC filter design is to avoid any interaction with the grid. This makes it important to model the impedance of the grid as seen from the converter station. When setting up a HVDC station, the project specification will detail the strength of the grid and also provide information about the impedance of the grid. It is valuable to include this in the filter design study to ensure that there is no resonance at frequencies where the harmonic currents are largest. However, in many cases it is difficult to define the grid impedance as it is constantly varying due to many factors such as the configuration of the network and load changes. A few methods have been developed to quantify the possible impedance scenarios that a converter station might deal with. One method is to cover a range of impedance values with a locus in the R-X plane so that all the data points for a range of frequencies are plotted [7]. This impedance-frequency locus is still subject to drastic changes due to the network conditions. A set of these harmonic loci can be enclosed in a larger sector or circle so that the

perimeter of the figure can be tested during the filter design process. The general sector model (Figure 2.13) is one of the methods of encompassing the impedance loci of the AC network. This is a worst case analysis which allows for a comprehensive design of filters. But this process could lead to over-design, in turn, increasing the cost and size of the harmonic filters. An alternative is to use an equivalent circuit that depicts the nature of the grid for most operating conditions by maintaining a constant impedance angle over the lower frequency range [8]. The CIGRE benchmark for a weak grid uses a simple voltage source behind an impedance of a resistive and reactive element with a SCR of 2.5 at 84 degrees.

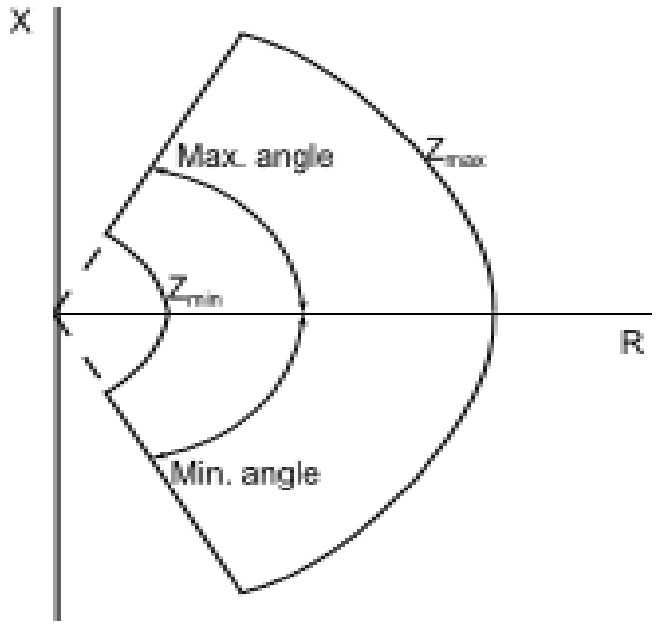

Figure 2.13: General Sector Model

For the preliminary frequency domain study, the general circle method (Figure 2.14) was used to identify possible conditions of resonance between the filters and the grid. There are three parameters that define the area of interest in the general circle model.

a. Radius – The radius of the circle defines the maximum possible magnitude of the AC network impedance and forms the perimeter of the figure.
b. R_{min} – This is the least possible resistance value of the grid. For any given condition, the resistance value cannot be lower than the minimum value given by R_{min}.
c. Maximum angle – This is the largest possible X/R ratio of the grid. Together with the R_{min} value, this makes the model a little more realistic and avoids overdesign to some extent.

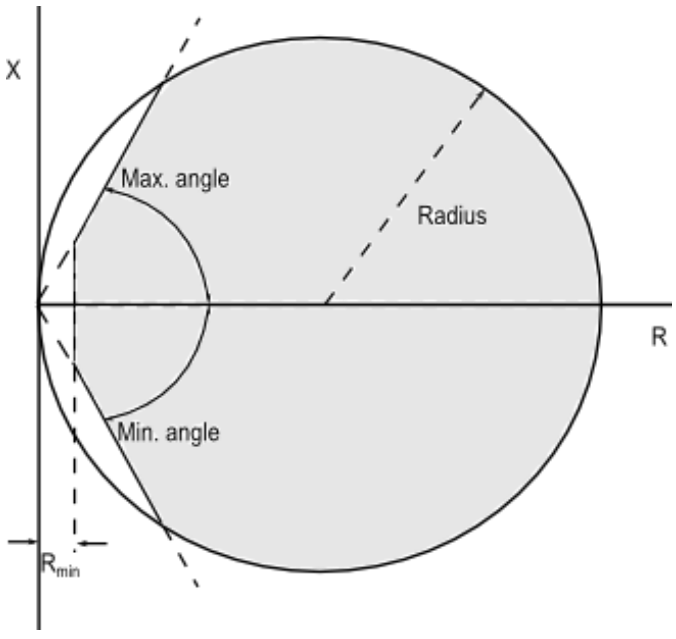

Figure 2.14: General Circle Model

By testing the filter impedance with the values on the perimeter of this figure it can be ensured that all values within the circle will also meet the desired harmonic performance specifications.

2.7 System Resonance Issues

Once the filter is designed based on the harmonic filtering and reactive power requirement, its impedance frequency characteristic can be created. The impedance model of the grid and filters is used to calculate the voltage and current values in the frequency domain. Due to the extreme variability of the grid, it is inevitable that resonant conditions occur between the filter and the grid. A parallel resonance is when the combined system impedance to the flow of harmonic current is very large. At lower orders the grid is usually inductive while the filters are capacitive which can cause harmonic current to circulate between them. For a strong grid, the parallel resonance will occur at higher frequencies which are beyond the harmonics of concern, but for a weak grid, parallel resonance is a major problem. On the other hand, series resonance is a low impedance path to the harmonic current which could result in amplification of voltage distortion at the PCC. These issues are the main reason why alternative strategies of filtering are investigated.

CHAPTER 3

HVDC System Design

In this chapter, the design process of the entire HVDC system is covered including the passive filters and the transformer. This forms the test system for the identification of the system resonance problem and further, the design of the Hybrid Active Filter to mitigate this situation.

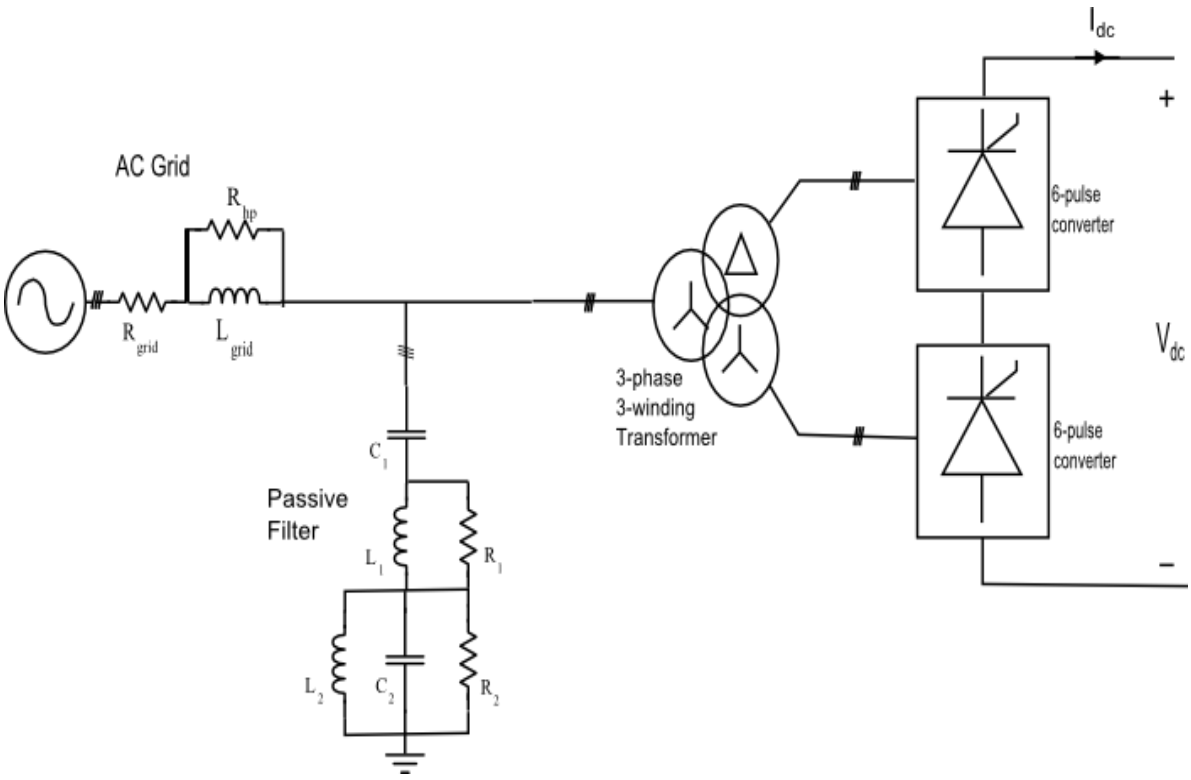

Figure 3.1: HVDC System

3.1 System specifications

There are various aspects of the HVDC system design process that begin with the specification of the AC system and the rating of the HVDC converter. According to the output requirements, the LCC operating point is chosen to design the parameters for the converter as well as the transformer. The filter design process involves identifying the harmonics created by the converter and then designing filters for those harmonics by following the harmonic performance analysis process described in the previous chapter. The specifications for the HVDC system are tabulated below.

Table 2: HVDC system specifications

AC network	
Voltage	345 kV (l-l, RMS)
Frequency	60 Hz
SCR	2.5
DC network	
Power	500 MW
Voltage	250 kV

3.2 LCC Design

The operation of an LCC has to be studied to identify the parameters to control the function of the converter. To understand the control variables it is important to derive the mathematical model that defines the function of the LCC. The work presented in [1] is briefly summarized in this section along with the equations for the output voltage and its

relationship to the input AC voltage, firing angle and overlap angle that are the result of that study.

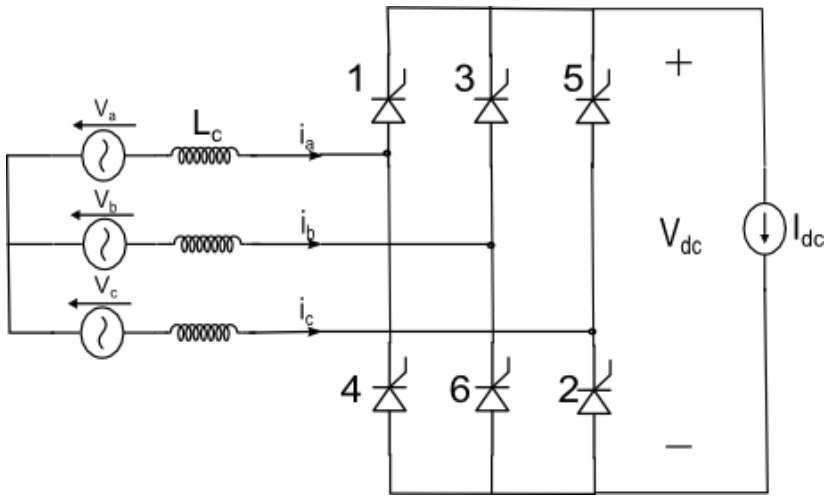

Figure 3.2: LCC circuit model

At any given instant, one thyristor of the upper commutation group (1, 3, 5) and one of the lower group (2, 4, 6) are conducting. Thus, the output DC voltage at any instant is one of the six possible line to line voltage combinations. The firing angle, α, controls the instant at which the DC voltage changes from one line voltage to another. If it is assumed that all six thyristors are fired at equal intervals then the DC voltage consists of six identical segments of 60 degrees width each. The average DC voltage can thus be found by averaging over any 60 degree interval of the voltage waveform.

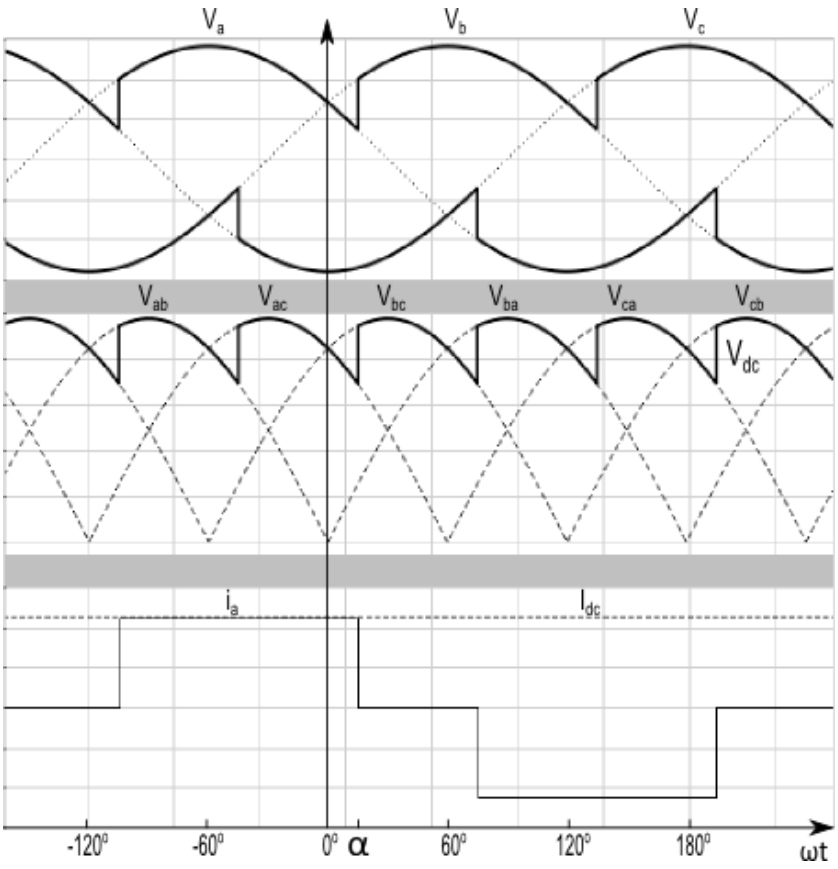

Figure 3.3: Ideal LCC voltage and current waveforms

The resulting equation from [1] for the DC voltage is

$$V_{dc} = V_{dio} \cos \alpha \qquad (13)$$

$$V_{dio} = \frac{3\sqrt{3}}{\pi} V_m \qquad (14)$$

where V_m is the magnitude of the input phase voltage.

In reality, once the firing command is given, the current in the commutating reactor cannot change instantaneously and a delay is introduced for the transfer of current from one

valve to another. This is called the commutation period and quantified by the overlap angle, μ. The operation of the LCC during the commutation period is seen in Figure 3.4.

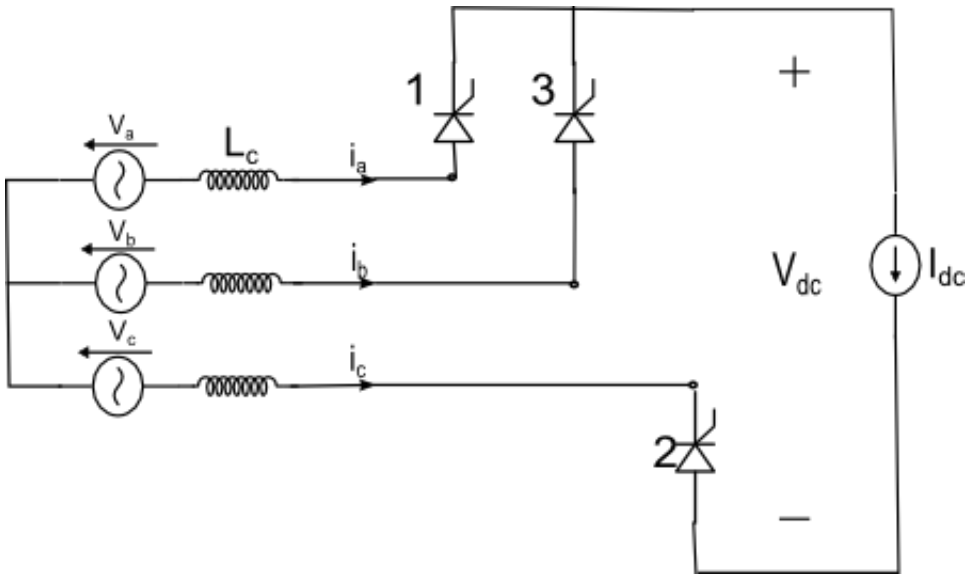

Figure 3.4: LCC circuit operation during commutation period

The effect of this commutation period is that the DC voltage is reduced due to the voltage drop across the line reactance. This drop is directly proportional to the DC current and the inductance of the commutating reactance.

$$\Delta V_{dc} = \frac{3}{\pi}\omega L_c I_{dc} \qquad (15)$$

The resulting voltage is then captured by the presence of the overlap angle in

$$V_{dc} = V_{dio}\frac{\cos(\alpha) + \cos(\alpha + \mu)}{2} \qquad (16)$$

The reactive power consumed by the HVDC converter due to the phase delay between the current and voltage waveforms is given by

$$Q_L = P_{dc} \tan\theta \qquad (17)$$

where $\cos\theta \approx V_{dc}/V_{dio}$ and $P_{dc} = V_{dc}I_{dc}$ can be substituted in (17) to get

$$Q_L = V_{dc}I_{dc}\sqrt{\left(\frac{V_{dio}}{V_{dc}}\right)^2 - 1} \qquad (18)$$

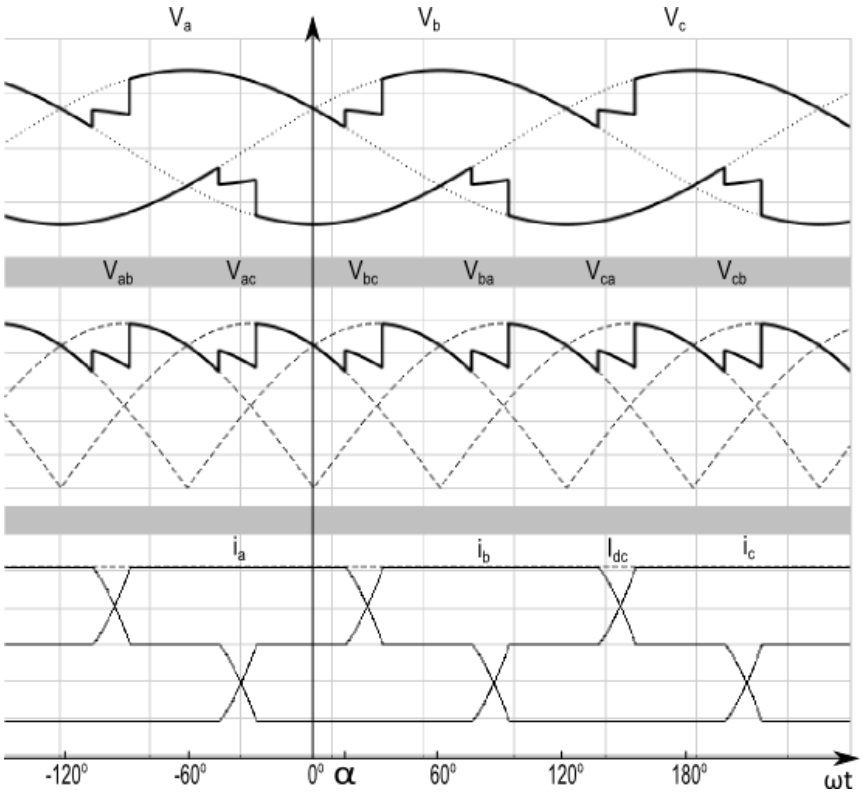

Figure 3.5: LCC voltage and current waveforms including effects of commutation

Using these equations, the commutation reactance and required input AC voltage can be calculated to get the required output DC voltage. However, the input AC voltage and the commutation reactance are both defined by the transformer turns ratio if the per unit leakage reactance of the transformer has already been specified. Thus, the design process becomes iterative with the inclusion of the turns ratio of the transformer. A simple algorithm can be written to solve for the parameters that would give the desired results. A script was written in MATLAB for this process.

3.3 Transformer Design

The transformer was specified to have a per unit leakage reactance of 12%. The transformer turns ratio is designed so that the required input voltage magnitude is available at the converter terminals so that it can function at the designed operating point.
As mentioned in the previous section, a MATLAB script was written to run an iterative design process to calculate the necessary turns ratio that fulfilled the condition of providing enough input voltage despite the voltage drop across the commutation reactance. The value of this reactance also depends on the turns ratio.

3.4 Phase Locked Loop

For a HVDC system the synchronization of the firing pulses to the commutating bus is very important to achieve the results modeled by the derived equations for the LCC operation. This is done by using a PLL to generate the phase of the commutating AC bus.

The voltage at the PCC is detected and a PLL circuit is used to track the phase of the voltage waveform. While using the PLL it is important to determine the order of the valve firing and extract the phase so that the voltage signals are aligned with the respective switches. The firing pattern and the respective positive line voltages are shown in Table 3.

Table 3: Thyristor valve firing pattern

Positive line voltage	Valve number
V_{ac}	1
V_{bc}	2
V_{ba}	3
V_{ca}	4
V_{cb}	5
V_{ab}	6

Thus, the PLL is controlled so that the phase output is aligned with the line voltage, V_{ac}, and the firing pulses are generated for the pattern listed in Table 3. The delta connected converter voltage has a phase lag of 30 degrees so the firing pulses must be shifted by 30 degrees to synchronize with the wye connected converter.

The synchronous reference frame (SRF) PLL is a widely used technique which extracts the phase by regulating the q-axis voltage to 0. More information about the convention of the SRF used can be found in Appendix A. The control diagram for the implementation of the PLL is seen in Figure 3.6.

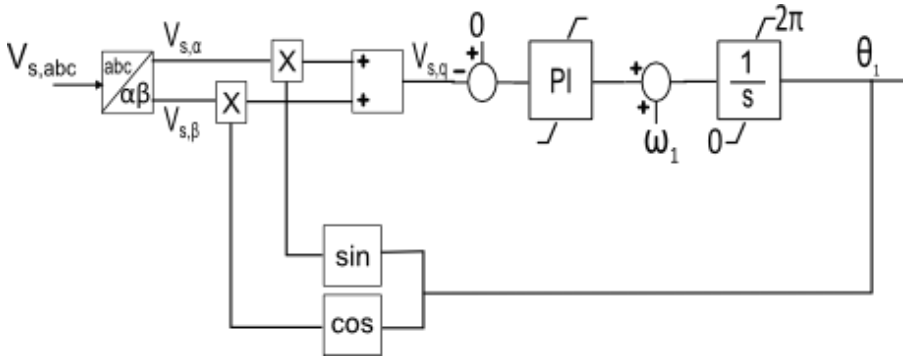

Figure 3.6: PLL control diagram

Here the term, ω_1, is the fundamental angular frequency added to specify the system frequency. The PI regulator sets the phase output to minimize the error and in the process controls the quadrature axis voltage to zero. The integrator wraps the values back to zero once it reaches 2π to keep the phase output between 0 and 2π. This serves as the feedback transformation angle to get the q axis synchronous reference frame value.

3.5 Initial Design Results

For the purpose of harmonic filter design, it is useful to analyze the worst case of harmonic generation by the HVDC converter. In HVDC converters used for power transmission the firing angle is controlled by the current or voltage regulators to ensure the proper operation and transmission of power between two networks. For a rectifier a smaller firing angle would give more DC voltage output and also require less reactive power. It is desirable to maintain a low firing angle but the normal steady state range for a rectifier is 10-18 degrees [9]. A firing angle of 18 degrees was chosen to ensure the filters were designed

for the worst case. The results of the design process for the LCC and transformer parameters were used to create a time domain simulation model in PSCAD. The grid was assumed to be an ideal voltage source to test the derived values. The simulation results are documented in this section that show the operation of the converter to supply the rated power at the rated DC voltage.

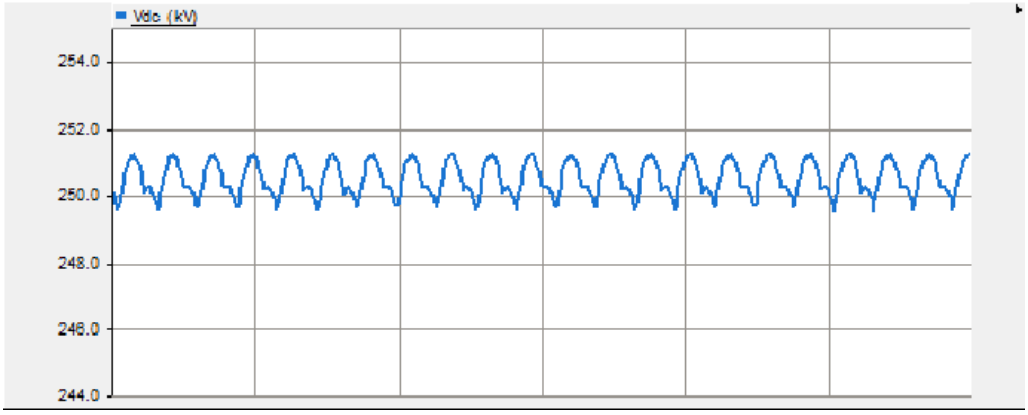

Figure 3.7: LCC direct voltage output

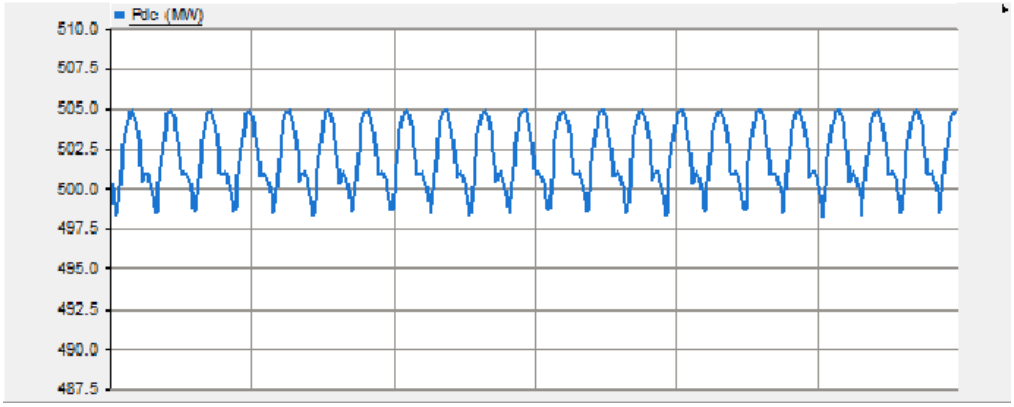

Figure 3.8: DC power consumed at the load

The results validate the design process and the parameters used for the HVDC system. However, without any filtering the grid supplies all the harmonic current that is required by the HVDC converter.

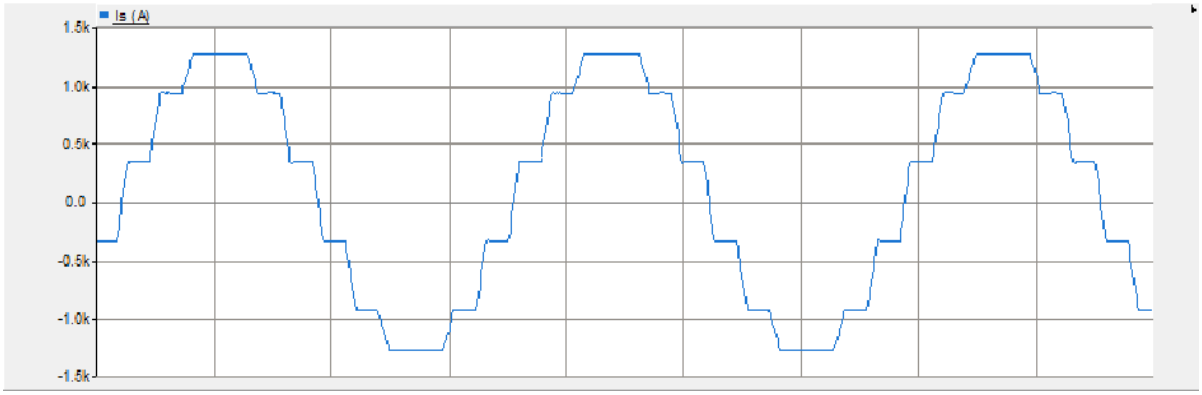

Figure 3.9: Source current for one phase

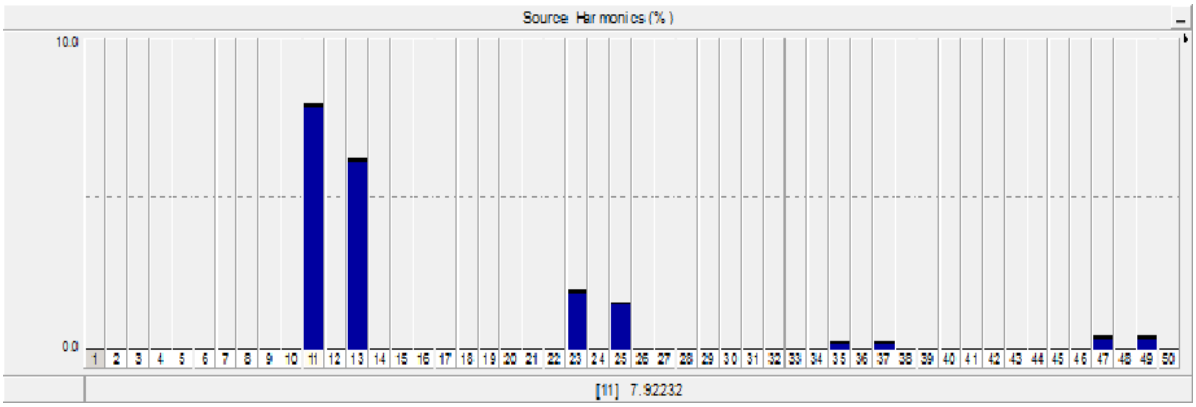

Figure 3.10: Source harmonic current magnitude

The phase current of the grid has very large amounts of harmonic current as can be seen in Figure 3.9 and Figure 3.10. The 12-pulse current waveform with the slope of the commutation period can be seen in Figure 3.9.

3.6 Passive Filter Design

As can be seen from the harmonic content in the source current, it is important to design passive filters that will sink the major harmonics {11^{th}, 13^{th}, 23^{rd}, and 25^{th}} and also provide some damping for the higher order harmonics. Considering the need for multiple harmonic filtering and also a high pass characteristic, the damped double tuned filter is a good candidate for the filtering. The filter must be tuned to remove the major harmonics from the grid. The damped double tuned filter also has a good bandwidth around the tuned frequencies. Hence, the filter is to be tuned to have low impedance at the 12^{th} and 24^{th} harmonics. The high pass resistor of the filter also provides better high frequency characteristics.

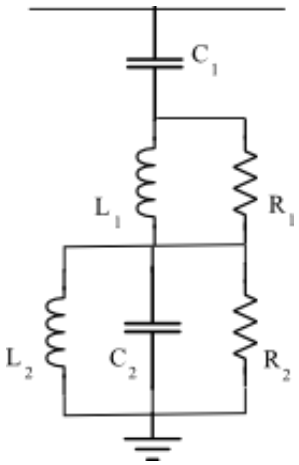

Figure 3.11: Damped double tuned filter

In creating a double tuned filter, the challenge is to choose values for the passive elements based on the reactive power requirement, tuning frequencies and damping resistors while ensuring that the performance matches the requirements. Each of these control parameters has a trade-off which makes the design iterative. The high voltage capacitor, C_1, has to be chosen to meet the reactive power requirements of the converter. Once this has been selected, the conventional double tuned filter design method is followed to select the values for the remaining reactive elements. The following equations were derived from the design process in [10] and [11].

$$C_1 = -\frac{Q_L}{V_s^2}\left(\frac{\omega_f}{\omega_s^2} - \frac{1}{\omega_f} + \omega_f \frac{\omega_1^2 + \omega_2^2 - \omega_s^2}{\omega_s^2\left(\omega_p^2 - \omega_f^2\right)}\right) \qquad (19)$$

$$L_1 = \frac{1}{\omega_s^2 C_1} \qquad (20)$$

$$C_2 = \frac{C_1}{\frac{\omega_1^2 + \omega_2^2 - \omega_p^2}{\omega_s^2\left(\omega_p^2 - \omega_f^2\right)} - 1} \quad (21)$$

$$L_2 = \frac{1}{\omega_p^2 C_2} \quad (22)$$

$$\omega_p \omega_s = \omega_1 \omega_2 \quad (23)$$

where ω_1 and ω_2 are the tuned frequencies, ω_s is the series resonance frequency of the circuit comprising L_1 and C_1, and ω_p is the parallel resonance frequency of the circuit comprising L_2 and C_2.

The parallel resonance frequency should be chosen to be between the tuned frequencies at a frequency where it is least likely for a harmonic current to occur so that no current or voltage amplification takes place. The damping resistor in the lower part of the filter branch, R_2, ensures that the parallel resonance impedance is limited to the value of the resistor. The upper damping resistor, R_1, provides the necessary high pass characteristic. However, there is a tradeoff between choosing a small resistor and the power loss due to higher harmonic current in that resistor. Through an iterative process the parameters for the damped double tuned filter were chosen (Table 4) and the frequency response of the designed filter is seen in Figure 3.12.

Table 4: Designed filter parameters

Passive element	Value
C_1	2.7012 μF
L_1	8.344 mH
R_1	400 Ω
C_2	5.9332 μF
L_2	4.463 mH
R_2	400 Ω

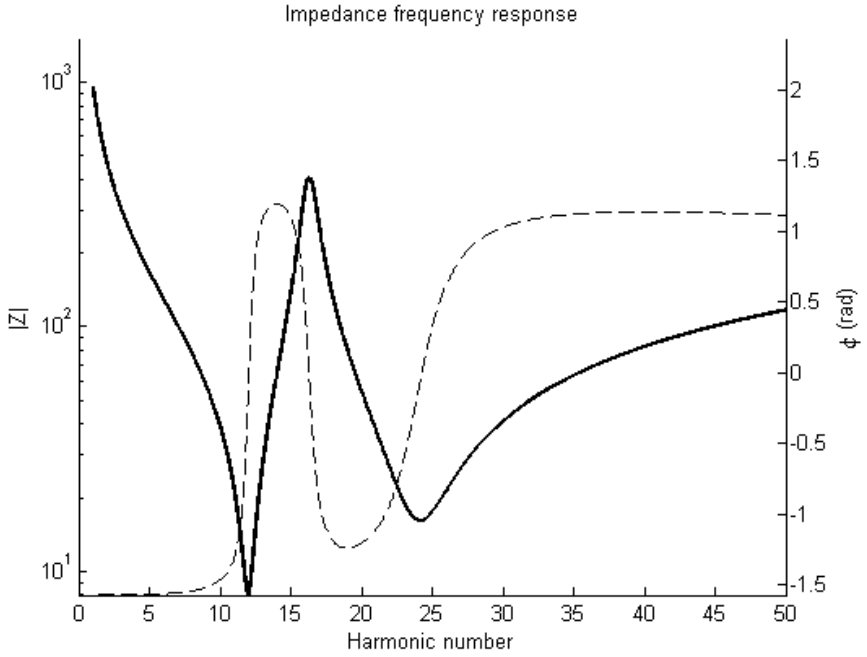

Figure 3.12: Filter impedance frequency response

3.7 PSCAD Results

The designed filter was then included in the PSCAD simulation and the AC grid was modeled as a weak grid of SCR 2.5 according to the CIGRE benchmark model for HVDC systems. It was seen that the filter was able to remove the harmonics seen in the previous

time domain simulation and the filter also provided reactive power compensation to the converter. Some of the reactive power support was provided by a capacitor bank which also drained some higher order harmonics due to its low impedance at high frequencies. The resulting three phase current waveforms for the system are seen in Figure 3.13 and their harmonic current magnitude plot is seen in Figure 3.14.

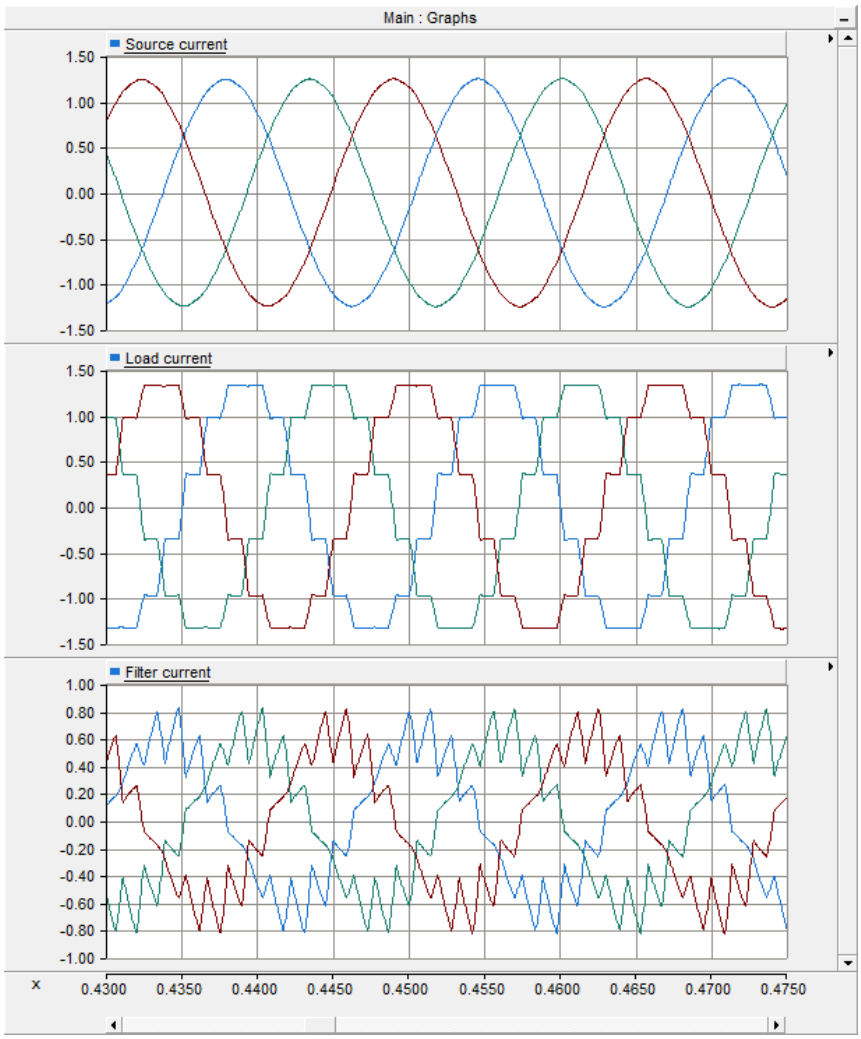

Figure 3.13: AC system three phase current waveforms

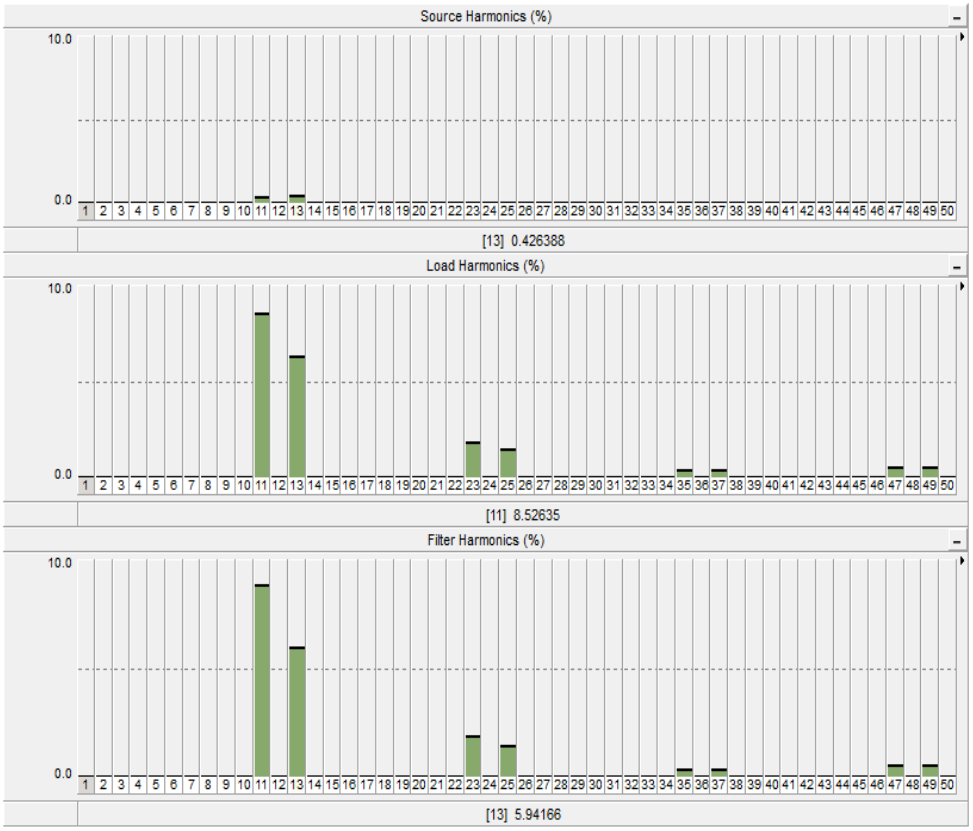

Figure 3.14: System harmonic current magnitude

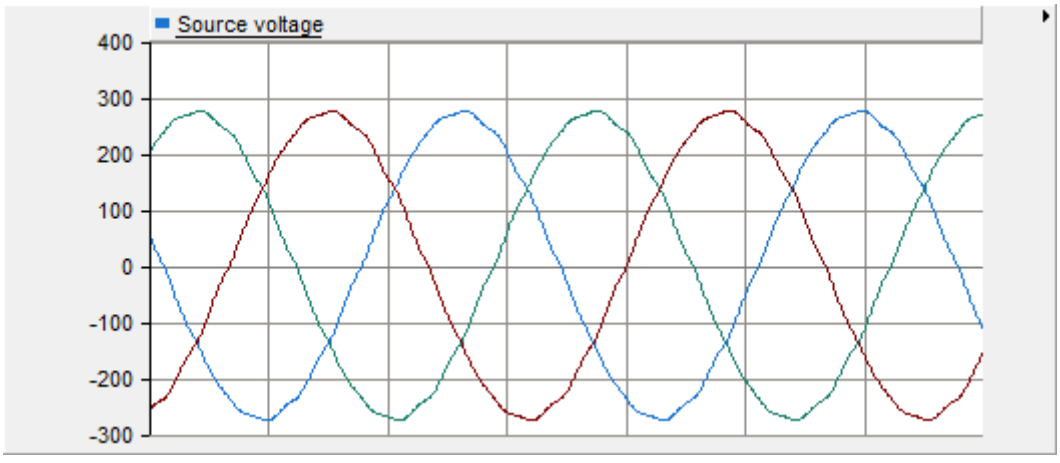

Figure 3.15: Grid voltage at PCC

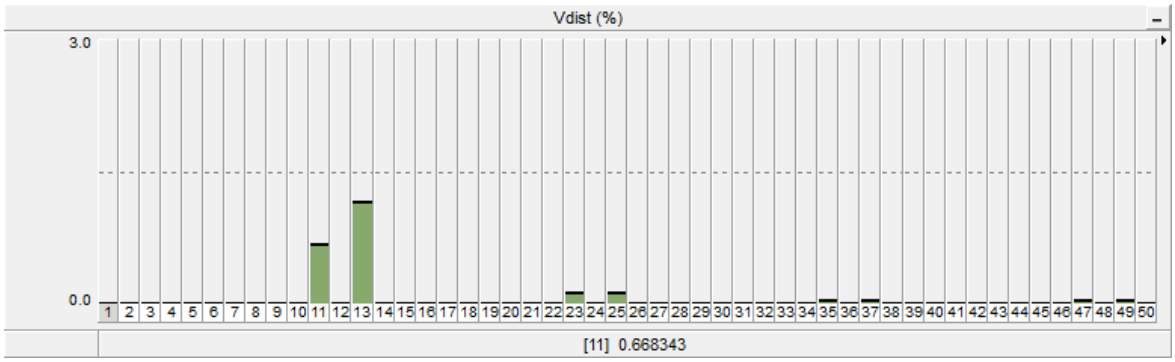

Figure 3.16: Individual harmonic voltage distortion

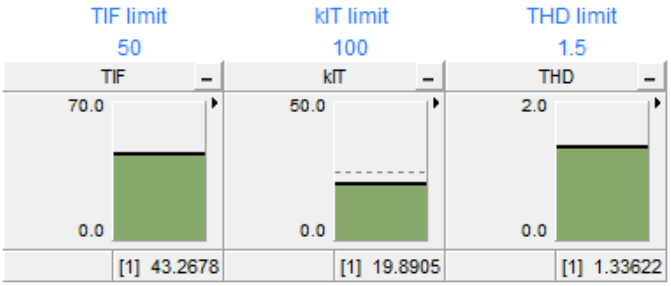

Figure 3.17: Harmonic performance specifications

The designed filter is able to meet the harmonic performance requirements and also provide the reactive power support to the HVDC converter. However, as discussed in Chapter 1, the grid is highly variable and can interact with the passive filter. Such a resonant condition can cause amplified harmonic currents in the grid.

3.8 System Resonance Analysis

In order to identify possible resonant conditions of the system, a frequency domain analysis was done using the harmonic system model introduced in Chapter 2. The converter was modeled as a harmonic current source and the general circle model was used for the grid. The harmonic values for the grid conditions were obtained from a consultant at General Electric. The designed filter was tested with all possible values on the perimeter of the grid impedance circle at each frequency to find the worst case resonance.

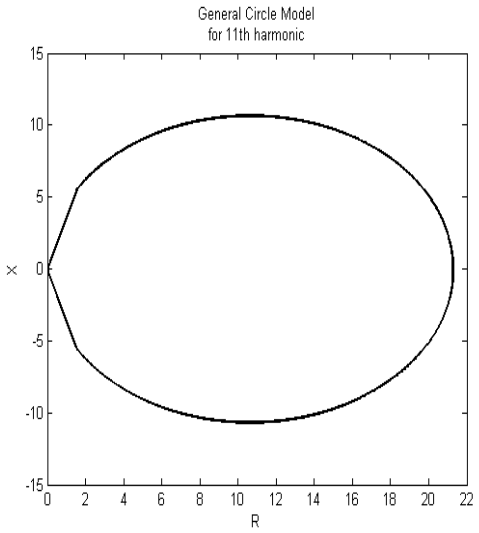

Figure 3.18: General circle model for a single harmonic frequency

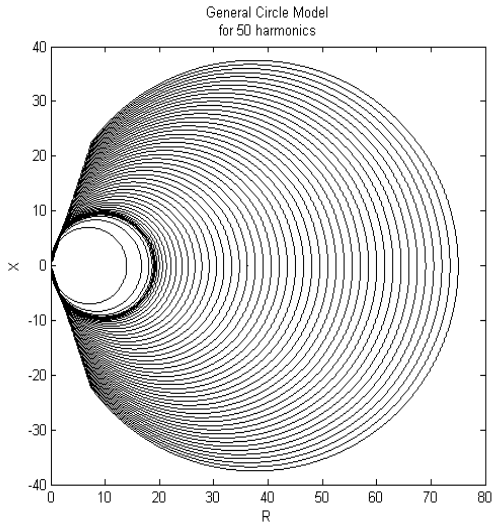

Figure 3.19: General circle model for harmonic number 2 to 50

The algorithm for the analysis found the worst cases of resonance at each harmonic frequency by solving for the voltage and current at the PCC for the combination of the filter impedance at that frequency with all possible grid impedance values as defined by the general circle. This is an extreme analysis since a grid condition that causes resonance at every harmonic is not realistic. However, it confirms the problem of resonance and stresses the need for prudent filter design as well as alternate solutions to filtering.

The bar graph in Figure 3.20 gives an indication of how the harmonic performance suffers during this resonance case. The normalized value in the figure is the multiple of the allowable limit.

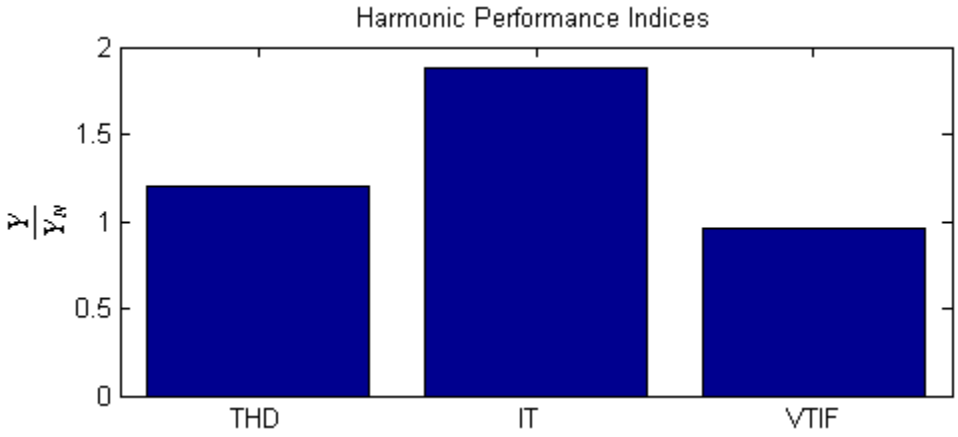

Figure 3.20: Harmonic performance indices

To get a more realistic view of the effects of grid resonance, a grid impedance that caused resonance at the 11th harmonic with the filters was identified using the MATLAB analysis and was used in a time domain simulation.

The impedance of the resonant grid from the MATLAB analysis was modeled after the AC network voltage source and a simulation was run to verify if the harmonic performance of the filters degraded because of resonance. The results showing the effect of the system resonance on the grid current are seen in Figure 3.21.

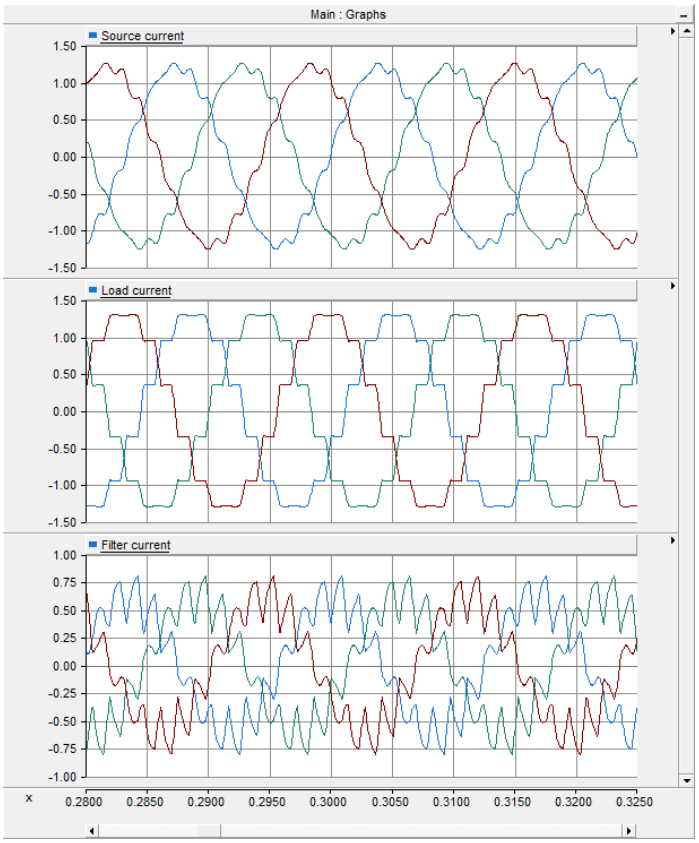

Figure 3.21: AC system currents due to system resonance at the 11th harmonic

Figure 3.22: Harmonic magnitude plot of the currents in Figure 3.21

The large values of the 11^{th} and 13^{th} harmonic currents are seen from the amplification due to the parallel resonance between the grid and the passive filters. This amplified current is circulated between the filters and the grid.

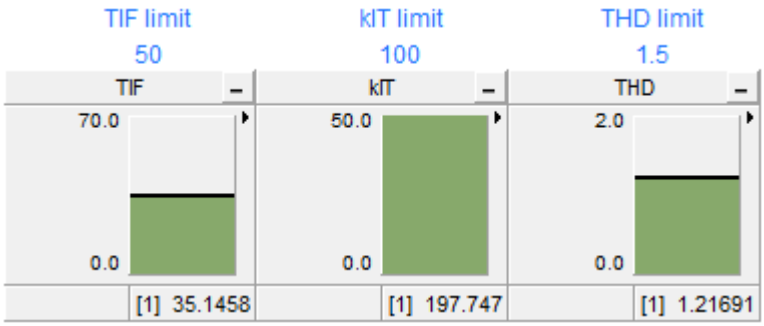

Figure 3.23: Harmonic performance indices during system resonance

Here the effect of resonance can be seen in current amplification. There is a large amount of harmonic current in the grid which is causing the IT value to go out of bounds as expected. The voltage distortion actually reduces due to this resonance effect. Thus, it can be seen that the passive filters are susceptible to resonance due to changing grid conditions and may not be sufficient in ensuring the filtering of harmonics from the network. For this reason, the concept of active filters was introduced.

CHAPTER 4

Active Filters

The inability of passive filters to guarantee harmonic filtering due to problems such as resonance with the grid and detuning has led to the use of active filters at non-linear loads. Passive filters also occupy a large area and have a significant cost. Besides, the design process for a passive filter is very complicated and relies on accurate data of the network conditions. The fact that a system evolves over time and is bound to change adds to the intricacy of passive filter design. This makes the active filter an option to consider for filtering harmonics for HVDC converters.

4.1 Background

An active filter cancels the harmonic content in the load by injecting harmonic currents with the same magnitude but opposite phase. The active filter first detects the amplitude and phase of the AC current harmonics and then creates the appropriate harmonic voltage to negate those harmonics. This is achieved by using an IGBT controlled VSC. The converter uses power from the AC system to function as an active harmonic source. Since the converter appears as a voltage source to the system, there is no interaction with the rest of the system unlike the passive filters.

Active filters have been proposed for a variety of industrial loads. One of the main considerations with active filters is the rating of the converter. Even with the vast

improvement in recent years, the IGBT is suited for low to medium voltage applications since it cannot block very high voltages. For this reason, the use of active filters for HVDC converters is limited.

4.2 Voltage Source Converters

The basic DC-DC converter principles form the base for the operation of the VSC. The main advantage of the IGBT is that it can be turned on or off with a gate signal whereas a thyristor is dependent on negative line voltage for turning off. Hence, it is possible to have complete control over the converter current which gives the VSC the ability to not only create any current profile but also to supply leading or lagging current which allows for control over the reactive power.

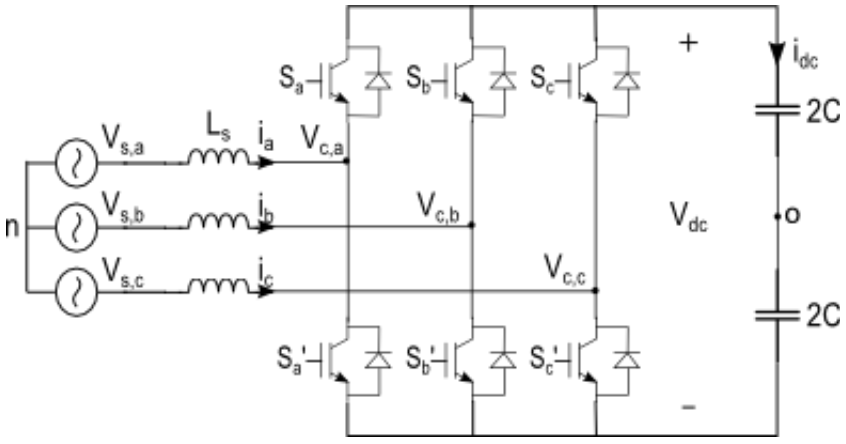

Figure 4.1: VSC circuit model

The VSC is termed so because it has a fixed DC voltage for both rectifier and inverter modes of operation. The thyristor based LCC has a fixed current polarity while the VSC can conduct current in both directions while maintaining a fixed voltage polarity.

The modeling of a VSC for the purpose of designing controls is investigated in the following section. A complete analysis involves the derivation of the converter transfer functions. These define the operation of the converter and are taken as the plant for which compensators are designed.

4.2.1 System Representation

The analysis of the converter operation is done to get equations to describe the system behavior and also create transfer functions that can be utilized with the control theory to design voltage and current regulators.

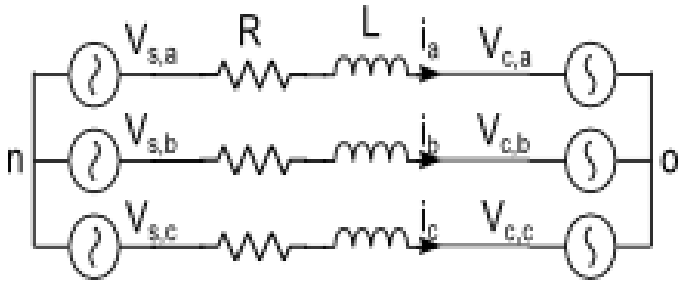

Figure 4.2: AC side VSC circuit model

The voltages, $V_{s,abc}$, signify the AC system to which the converter is connected, the phase currents, i_{abc}, flow into the converter through the inductor, L, and the input converter voltage is $V_{c,abc}$. This voltage is with respect to the point 'O' which equally divides the DC

link voltage. The analysis presented considers phase voltages and the loss in the inductor is modeled as a resistor, R. An in-depth derivation of the system equations can be found in [13]. Following the rules of Kirchhoff's circuit laws we get

$$v_{s,abc} = v_{c,abc} + L_s \frac{di_{abc}}{dt} + Ri_{abc} \qquad (24)$$

The p-q theory introduced in [14] allows instantaneous compensation of reactive power in three phase circuits and for non-linear loads. The three phase equations are transformed to the rotating reference frame according to this theory. The use of the synchronous dq reference frame allows decoupled control of active and reactive power flow [12]. The basis for this transformation is found in Appendix A. The convention chosen for the dq transformation is that the direct axis controls real power and the quadrature axis controls the reactive power. (Eq. 24) is transformed to the synchronous reference frame to get

$$v_{s,d} = v_{c,d} + L\frac{di_d}{dt} - \omega L_s i_q + Ri_d \qquad (25)$$

$$v_{s,q} = v_{c,q} + L\frac{di_q}{dt} + \omega L_s i_d + Ri_q \qquad (26)$$

The objective of deriving these equations is to control the converter voltage by creating a current reference. Hence, the system voltage and cross-coupling inputs to this equation are compensated through feed-forward, and the Laplace transformation of (26) gives a relationship between the current and the converter voltage.

$$\frac{i_{d/q}}{v_{cd/q}} = -\frac{1}{sL_s + R} \qquad (27)$$

This transfer function is used as the plant in control theory and a current compensator is designed to regulate the converter output voltage. The negative sign of the transfer function comes from the convention of measuring current going into the converter as positive. If the opposite convention is used then this sign will disappear.

For the DC link voltage control, the power balance theorem can be used to derive the equations for the DC side of the converter. Assuming no losses in the switches and the inductor, the power from the AC system, P_{src}, must equal the power delivered to the DC load, P_{load}.

$$P_{src} = P_{load} \tag{28}$$

From the IRP theory, we have

$$P_{src} = \frac{3}{2}\left(V_d I_d + V_q I_q\right) \tag{29}$$

and according to the chosen convention for the SRF, $I_q = 0$ since it does not contribute real power. Thus, we get

$$P_{src} = \frac{3}{2} V_d I_d \tag{30}$$

and

$$P_{dc} = V_{dc}^{*} I_{dc} \tag{31}$$

where Vdc^{*} is the reference DC voltage. Substituting (30) and (31) in (28) we can derive the equation for the DC link operation of the converter where

$$I_{dc} = C\frac{dV_{dc}}{dt} \tag{32}$$

$$\frac{3}{2}V_d I_d = V_{dc}^* C \frac{dV_{dc}}{dt} \qquad (33)$$

Here V_d is the direct axis voltage of the AC system to which the converter is connected and C is the DC link capacitance. Taking the Laplace transform and rearranging we get,

$$\frac{v_{dc}}{i_d} = \frac{2 * Vdc}{3 * Vd} \frac{1}{sC} \qquad (34)$$

This is the transfer function for which the voltage regulator will be designed that will output a current reference for the current regulator.

4.2.2 Control Design

The control objectives for a VSC can vary depending on the application of the converter. For power control a current reference can be generated by doing the required arithmetic to solve for the reference to the current regulator which will generate the necessary converter voltage to meet the power requirement. In the rectifier mode, the goal of a converter might be to maintain DC link voltage. Here a DC link voltage controller creates the current reference for the current controller to achieve the desired DC voltage. The current control forms the inner loop and has a high bandwidth controller which makes it faster than the outer loops that generate the reference. An overview of the control diagram for DC link voltage control is seen in Figure 4.3.

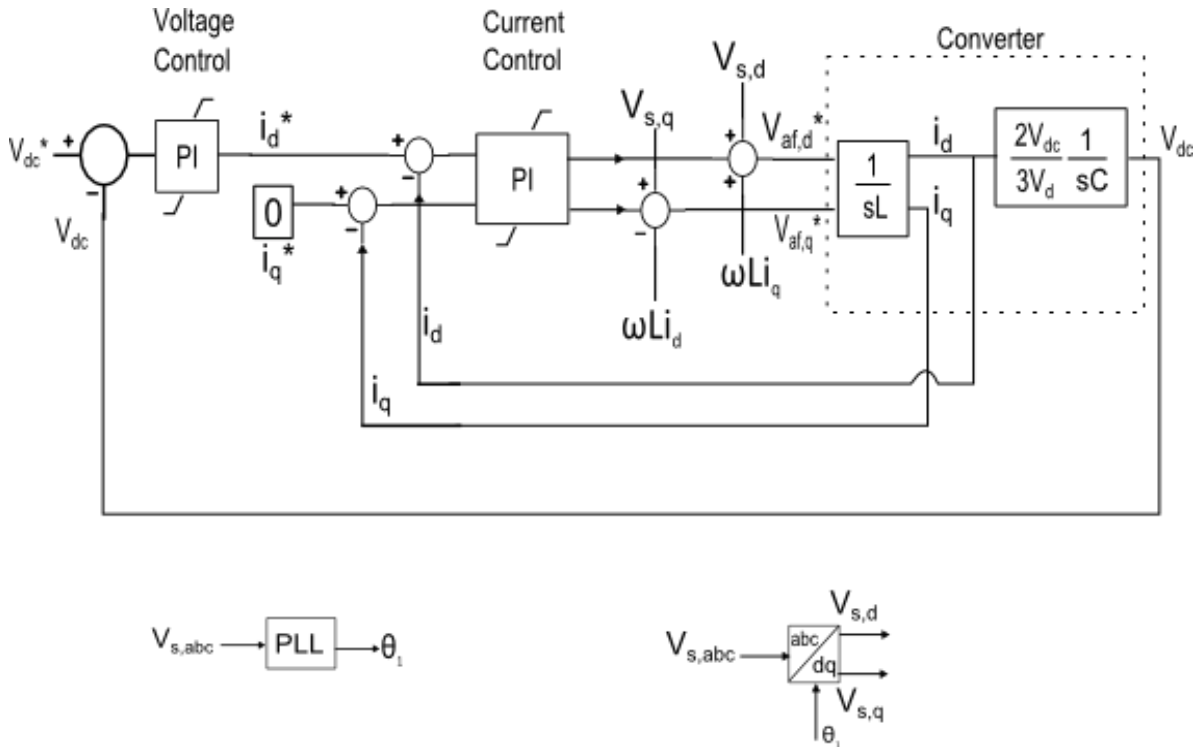

Figure 4.3: Control diagram overview for DC link voltage control

The converter is modeled in the control diagram with the system transfer functions. The controller output signals, $V_{af,d}$* and $V_{af,q}$*, are then transformed back to three phase signals and divided by $\frac{2}{V_{dc}}$ to get the modulating signal for the sine-triangle PWM technique of pulse generation. The modulating signal is compared with a high frequency carrier signal to create the pulses for the IGBTs.

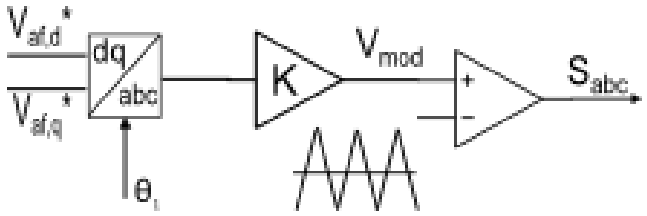

Figure 4.4: Sine-triangle PWM generation

These pulses are supplied to the gates of the switches to control the converter operation. If instantaneous real or reactive power control is desired then another outer PQ control loop will create a current reference which can be added to the reference created by the DC link voltage regulator.A big challenge in control design is to design the gains of the current and voltage regulators. The next two sections present a summary of the design of PI controllers the details of which can be found in [14].

4.2.2.1 Current Regulator

The current compensator controls the current going into the converter to regulate the converter voltage. The relationship between the current and the voltage of the converter was derived in the previous section to get the transfer function

$$\frac{i_{d/q}}{v_{cd/q}} = -\frac{1}{sL_s + R}$$

which is the plant for the control design model. This transfer function has a pole that must be cancelled using the zero of a PI compensator. The tuning of the proportional and integral gain by the technical optimum gain tuning method can be set as

$$K_p = L\omega_{bw} \qquad K_i = R\omega_{bw} \qquad (35)$$

The bandwidth of the regulator, ω_{bw}, can be chosen depending on the switching frequency and the feedback measurement delay. The MATLAB sisotool is also a valuable tool in designing the controller gains according exact response requirements.

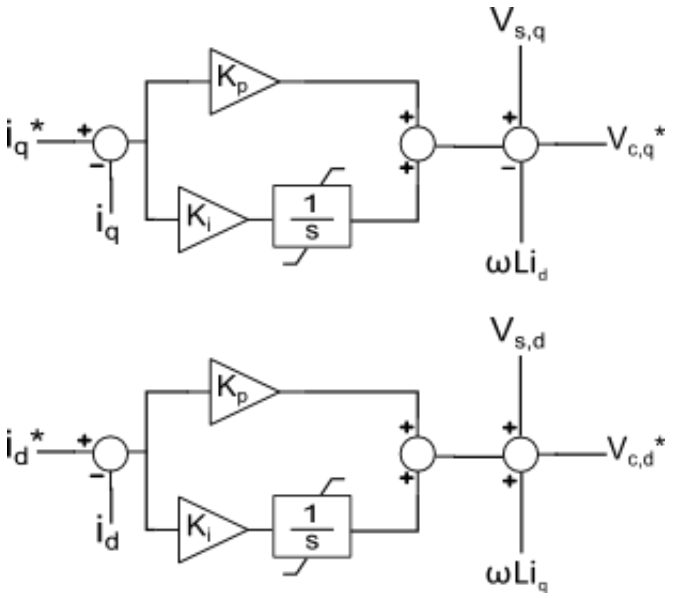

Figure 4.5: Current regulators in the SRF

The simplicity and zero steady state error of the PI regulator in the SRF with the feed-forward terms make it a good choice for controlling the current.

4.2.2.2 DC Link Voltage Regulator

The DC link voltage increases when the active power from the AC source is provided to the DC bus. The relationship between the current and the DC voltage was derived using

the power balance theorem previously. In [14] a second order nonlinear relationship is derived to calculate the gains for the PI regulator.

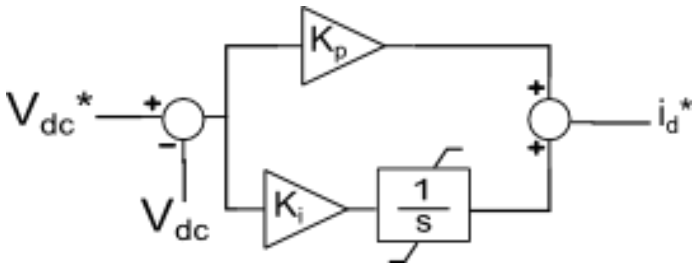

Figure 4.6: Voltage control using PI regulator

The result from [14] for the frequency domain analysis used to derive the gains is

$$\frac{V_{dc}}{V_{dc}^*} = \frac{\omega_n^2}{s^2 + 2\zeta\omega_n s + \omega_n^2} \qquad (35)$$

$$K_p = \frac{2\zeta\omega_n C V_{dc}^*}{\frac{3}{2}V_m} \qquad K_i = \frac{\omega_n^2 C V_{dc}^*}{\frac{3}{2}V_m} \qquad (36)$$

Where ω_n stands for the natural undamped frequency and ζ stands for the damping factor. With these gains the bandwidth of the regulator is given by

$$\omega_{bw} = \omega_n\sqrt{(1 - 2\zeta^2) + \sqrt{4\zeta^4 - 4\zeta^2 + 2}} \qquad (37)$$

A good phase margin can be obtained by setting the damping factor ζ above unity. This prevents overshoot and increases stability of the system. With a ζ value of 1.2 the bandwidth of the control is half of the natural undamped frequency ω_n. The output of this compensator

forms the reference to the direct current regulator. As a rule of thumb, the bandwidth of the outer loop DC link control can be around one sixth of the inner current controller bandwidth.

4.3 Active Filter Topologies

Depending on the way the VSC is connected to the system the converter can operate as a series active filter or a shunt active filter. These are the two topologies of the pure active filter connected to a system that has a nonlinear load.

4.3.1 Series Active filter

In this filtering method, the active filter is tapped from a transformer connected in series with the ac line. The converter is controlled to inject voltages that cancel out the distortion present in the system. Thus the source voltage remains distortion free.

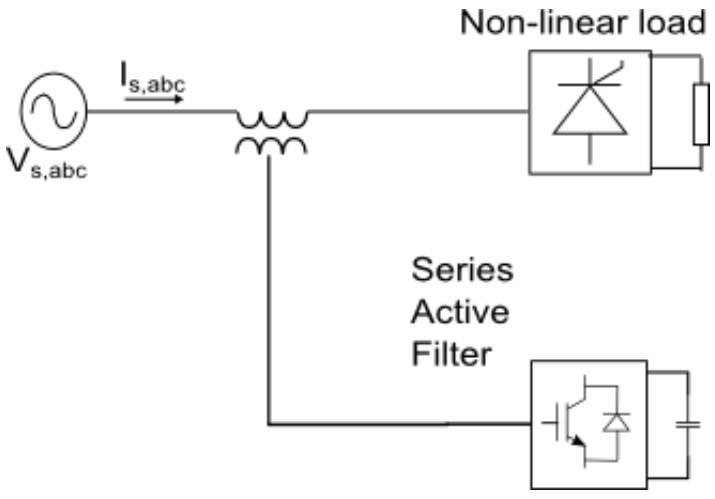

Figure 4.7: Series active filter

The problem with the series active filter is that all the fundamental current that flows through the transformer to the load has to go through the active filter as well which significantly increases the rating of the filter. It is certainly not a feasible option for the high voltage and current ratings of HVDC. However, it can be used as a filtering solution for small and even medium voltage applications.

4.3.2 Shunt Active filter

In this configuration the active filter is connected to the PCC in parallel with the load. A step down transformer is needed to reduce the voltage at the converter. Similar to the series active filter, the shunt active filter detects the harmonics in the load current and injects the opposite phase current to eliminate any high frequency current from the source. Since the transformer is not connected in series with the line, the converter does not have to conduct all the fundamental current. However, because of the leakage reactance of the transformer and the high turns ratio required to sufficiently step down the voltage at the converter, a magnified fundamental current can go through the IGBTs of the shunt connected filter.

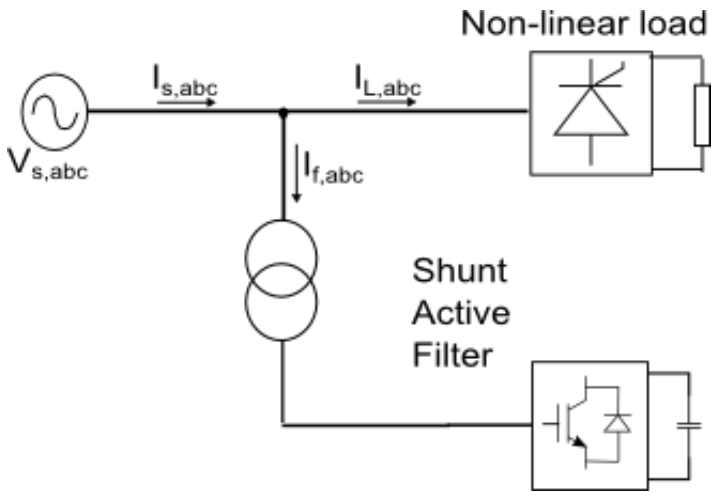

Figure 4.8: Shunt active filter

The control for the converter can also be made to sense the harmonics in the source current and then cancel them out. One implementation of the control for an active filter is seen in Figure 4.8.

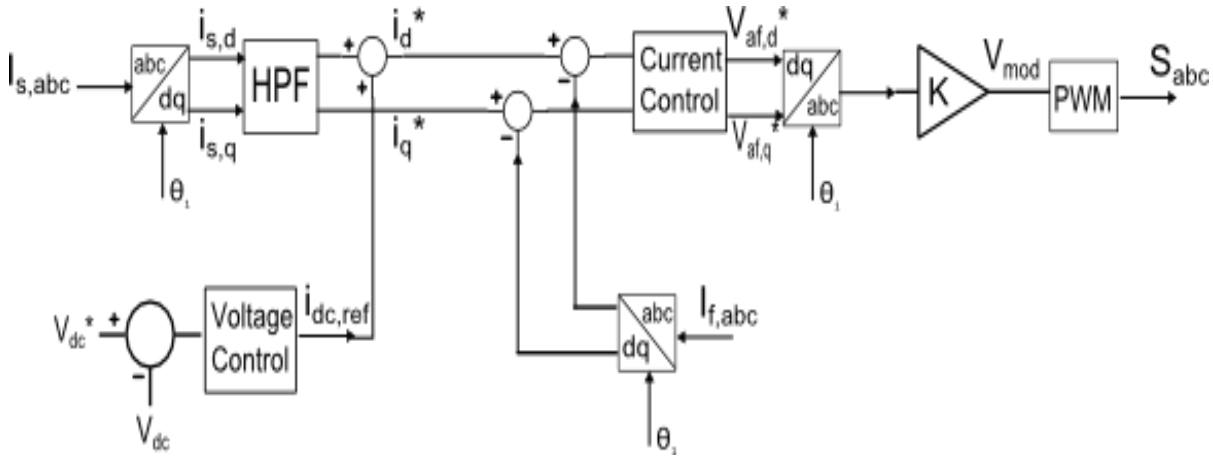

Figure 4.9: Harmonic current control for shunt active filters

The low frequency component of the source current is removed to form the reference for the converter current control along with the reference created by the DC link voltage control. This way the converter voltage can be regulated to inject the required harmonics. However, as noted before, a lot of fundamental current can flow through the converter due to the transformer leakage reactance. Considering that the converter is connected to the PCC, there is also a reasonable fundamental voltage in spite of the step down transformer. This greatly increases the power flow through the converter and also the converter rating.

To make these active filters economically feasible, the fundamental current has to be diverted through another branch. This idea is the motivation for the hybrid active filter topology. A few hybrid active filter configurations will be looked at in Chapter 5 along with the implementation of a unique configuration.

CHAPTER 5

Hybrid Active Filters

5.1 HAF Review

Due to the rating problems of the pure active filter, it cannot be utilized for HVDC systems where the voltage and current ratings are extremely high. For this reason, various HAF topologies [20] have been proposed. The motivation for having a HAF is to reduce the rating of the active filter either by diverting the fundamental current away from the active filter and minimizing the fundamental voltage seen by the converter.

One implementation of a shunt connected hybrid active filter that improves the performance of single tuned passive filters from [21] is discussed here.

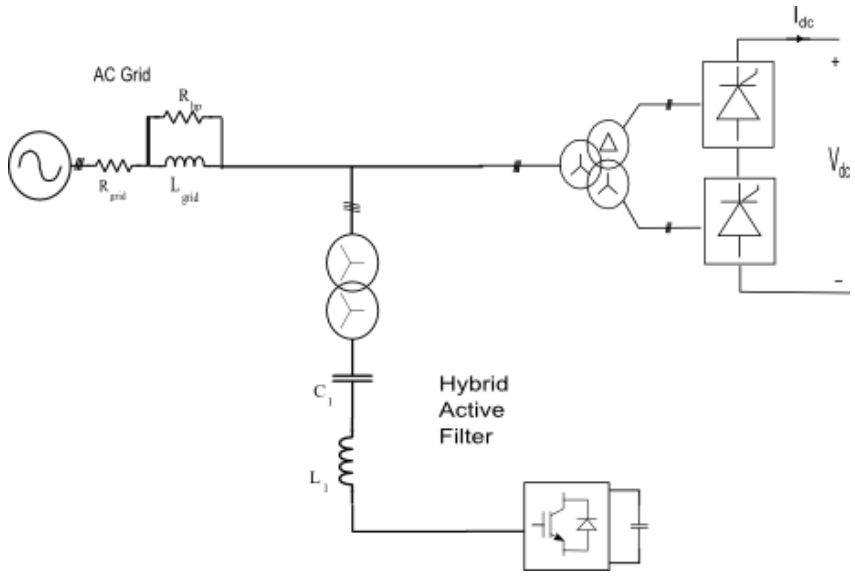

Figure 5.1: Dominant harmonic HAF

A passive branch is added in series with the shunt connected converter. The passive branch is tuned to provide a low impedance path at the tuned frequency allowing the converter to inject the required harmonics currents. However, the passive branch can be tuned to only one frequency which makes the active filter function limited to the filtering of a single frequency. It might be desirable to employ such HAF for the dominant harmonics as these filters provide the benefit of addressing variability around the tuned frequency as opposed to single tuned passive filters that also suffer from the effects of detuning and resonance. Another advantage is that the passive filter capacitor supports the fundamental voltage which reduces the voltage rating of the converter and the impedance to the fundamental current is also high as the passive branch forms a band pass filter. The control of this converter is done in the SRF by rotating the three phase reference current at the frequency of compensation to extract the harmonic reference.

5.2 Proposed HAF Topology

The HAF discussed in the previous section is effective to improve the performance of a single tuned filter. However, it still requires multiple HAFs to address the dominant harmonic currents as well as a high pass filter for the higher order harmonics. It was seen that the double tuned filter provided many advantages over the single tuned filter when considering passive filter design. The damped type of double tuned filter also had a good high frequency impedance characteristic. Thus, a hybrid filter topology is considered where

an active filter is connected to a shunt attached double tuned passive filter. This filter configuration allows active filtering of the dominant harmonics when needed.

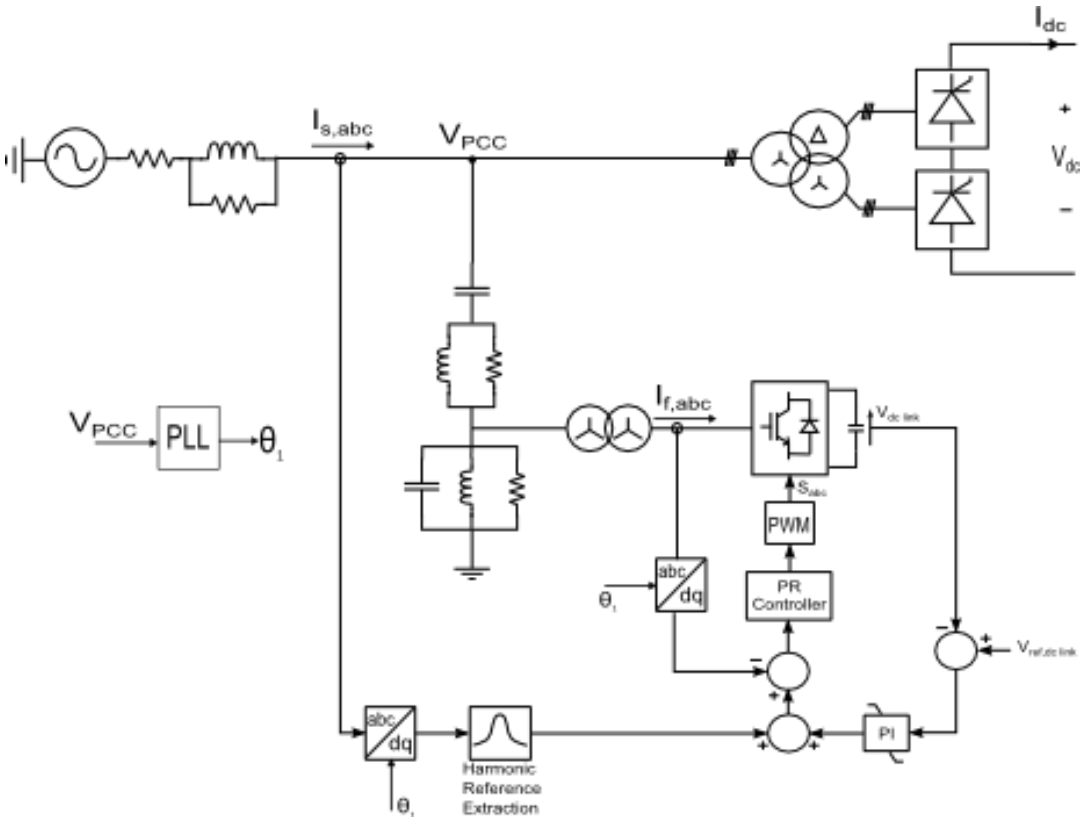

Figure 5.2: Proposed HAF Topology

Some of the advantages of this topology are listed below –

a. **Filtering for all harmonics of concern** - The passive filter is tuned to the 12^{th} and 24^{th} harmonics to provide effective filtering of the dominant 11^{th}, 13^{th}, 23^{rd}, and 25^{th} harmonics along with a low impedance path for the higher order harmonics.

b. **Lower rating of active filter** – The lower portion of the filter branch provides low impedance for the fundamental current so that the fundamental voltage across that segment of the passive filter is small. This reduces the voltage rating of the active filter which is connected in parallel with the lower branch and also requires a smaller turns ratio for the transformer. Also, the fundamental current is diverted through this passive branch which reduces the power rating of the active filter.

c. **Reactive power support** – The high voltage capacitor of the high pass branch of the passive filter supports all the fundamental voltage and also provides reactive power support to the HVDC converter.

d. **Active filtering at dominant harmonics** – The lower portion of the passive filter has a parallel resonance close to the 11^{th} and 13^{th} harmonics which enables the active filter to inject currents at those frequencies back into the grid through the high pass portion.

e. **Resonant condition harmonic compensation** – The active filter can share the load of the dominant harmonics which makes this HAF effective even if the passive filter and the grid create a resonance.

Hence, the hybrid active filter topology allows the voltage source converter to have a lower rating and provide the passive filter with filtering support. In case of detuning of the passive elements, the active filter can provide the necessary dominant harmonic compensation. This HAF is based upon the topology proposed in [22].

A major challenge with the proposed HAF is the design of the controls due to the complexity of selecting two harmonic currents for compensation while maintain the DC link voltage which requires fundamental current. The control design process is investigated in the following section.

5.3 Control Design

According to the HAF design, it is expected that the active filter provide compensation for the 11^{th} and 13^{th} harmonic currents which are the dominant currents injected by the HVDC converter while maintaining the DC link voltage. The SRF technique of harmonic selection employed in [23] is useful for compensation of a single frequency current. It transforms the three phase reference current by rotating at the frequency of compensation. However, this cannot be replicated for the proposed HAF because references generated for two distinct harmonics, by rotating at two different frequencies, cannot be added in the SRF to create a common reference current. Thus, the PR controller in [24] is implemented with this HAF.

5.3.1 PR Regulator Design

In [24] the PR regulator is developed in the stationary frame as an equivalent compensator to the PI regulator in the synchronous reference frame. This PR regulator can achieve zero steady state error without requiring complex transformations of a synchronous frame regulator. The ideal form of the PR controller is given by the transfer function

$$G_{AC}(s) = K_p + \frac{K_i}{s^2 + \omega_n^2} \qquad (38)$$

Here the controller has unlimited gain at the natural undamped frequency, ω_n. Thus, this can be used to directly control the AC signal. However, the infinite gain could cause stability problems and due to the practical limitations of signal processing, a damped form of the resonant controller transfer function is used.

$$G_{AC}(s) = K_p + \frac{2K_i\omega_c s}{s^2 + 2\omega_c s + \omega_n^2} \qquad (39)$$

$$where\ \omega_c = \zeta\omega_n$$

The damped frequency, ω_c is the bandwidth around the natural frequency and can be controlled by the damping ration ζ. Even though the gain is finite at ω_n, it is tuned to be large enough to eliminate all steady state error. The controller bandwidth can be increased by introducing more damping.

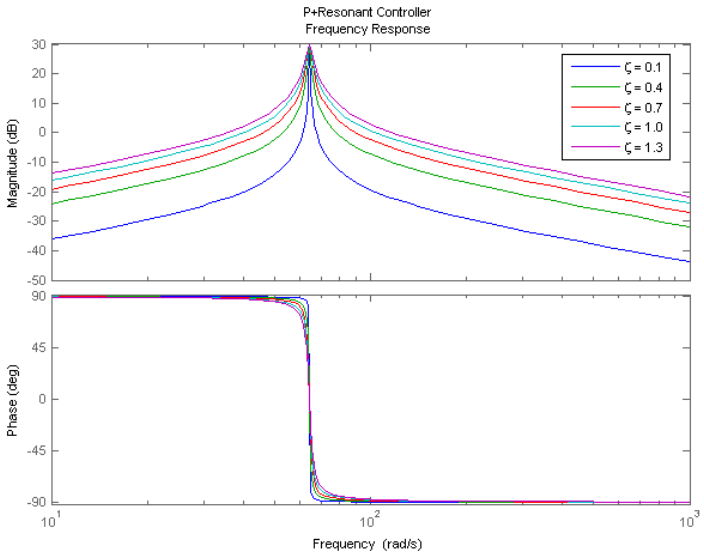

Figure 5.3: Resonant controller Bode plots for different damping ratios

5.3.2 PR Regulator in the stationary frame

In order to utilize the PR controller, the harmonic reference current must be extracted using a band pass filter with unity gain. The filter transfer function matches the resonant controller transfer function with the absence of the gain K_i. After the harmonic current extraction, the reference is transformed to the stationary αβ frame to control the AC signal, although the transformation is not required to utilize the PR controller. The advantage of converting to the stationary frame is that only two controllers are required, one for the α axis current and the other for the β axis current, whereas three controllers are required in the three phase system.

The control was tested for a non-linear load in the form of a three phase diode rectifier which is connected to an AC system modeled as an ideal three phase voltage source (Figure 5.4). The converter is controlled to remove the 5^{th} and 7^{th} harmonics from the source current.

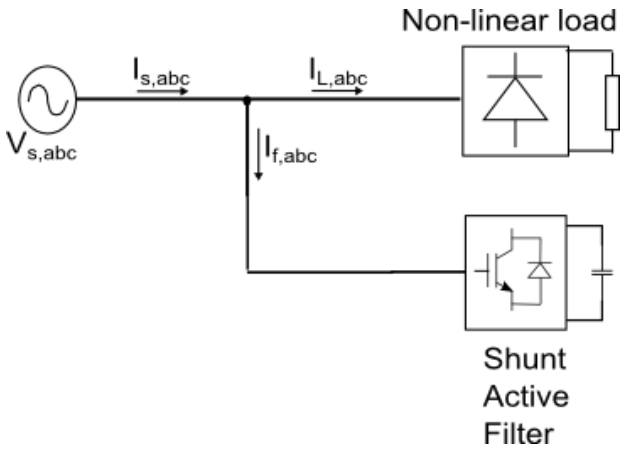

Figure 5.4: Test system for PR controller design

The results of using the PR regulator in the stationary frame to control the active filter current are seen in the plots in Figure 5.5.

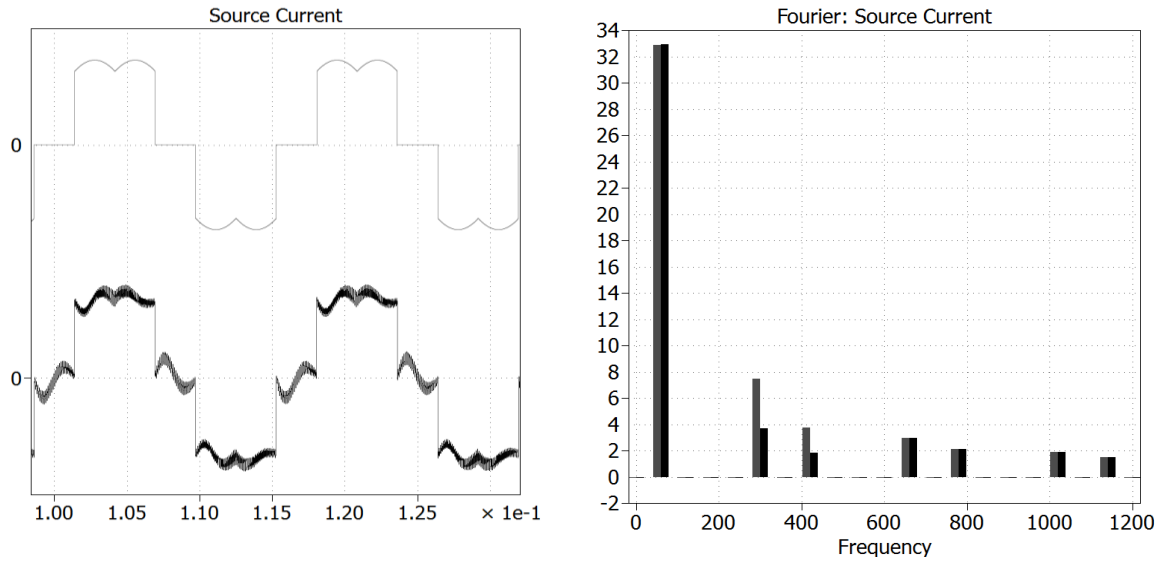

Figure 5.5: a) Source current waveform without (on top) and with active filter, b) Harmonic magnitude without (left) and with active filter

The 5^{th} and 7^{th} harmonics are significantly reduced by employing the PR controller for the active filter. The tracking of the generated reference is also quite accurate with no steady state error as can be seen in Figure 5.6.

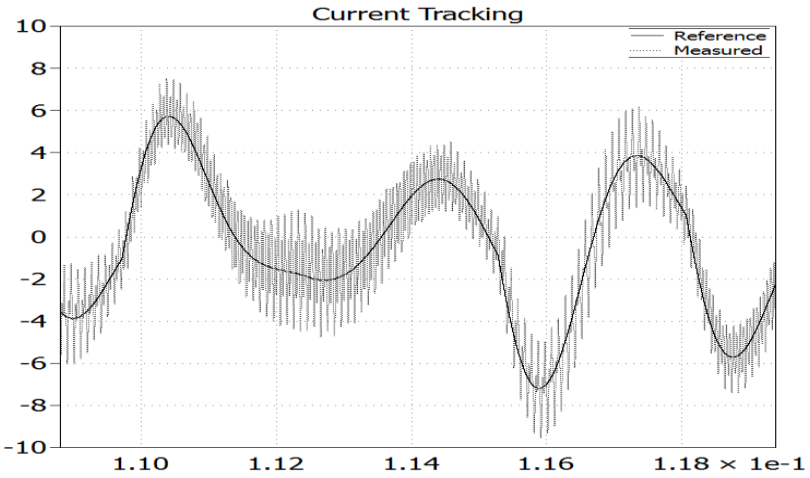

Figure 5.6: Reference current tracking using PR regulator in stationary frame

However, the PR controller in the stationary frame requires a regulator for each harmonic that is to be compensated.

5.3.3 PR Regulator in the synchronous reference frame

The PR controller employed in the SRF is equivalent to the conventional PI controller implemented in the SRF, separately for the positive and negative sequences. For instance, a twelfth harmonic PR regulator can control both the eleventh and thirteenth harmonic currents. By rotating at the fundamental frequency from the three phase reference to the SRF, the eleventh and thirteenth harmonic appear as the twelfth harmonic in the dq reference frame. This forms the reference to the PR controller which regulates the active filter current and in turn, compensates for both the eleventh and thirteenth harmonics. Thus, only one controller is needed for the control of currents at two different frequencies. The same can be

done for higher order harmonics, if needed, with the addition of a PR controller tuned at the 6^{th}, 18^{th}, 24^{th}, 30^{th} and so on.

When the SRF transformation is done the positive and negative sequence elements are accumulated at the zero sequence harmonic. For instance, the 5^{th} harmonic negative sequence current and the 7^{th} harmonic positive sequence current are rotating at the 6^{th} harmonic relative to the frequency of rotation of the SRF. Thus, after the rotation, the 6^{th} harmonic current can be extracted using a band pass filter to generate the reference for the PR controller in the SRF. The controller then regulates the AC signal to match the reference and the result is that both harmonics of concern are addressed. The results of the PR regulator for the test system of Figure 5.4 are shown below.

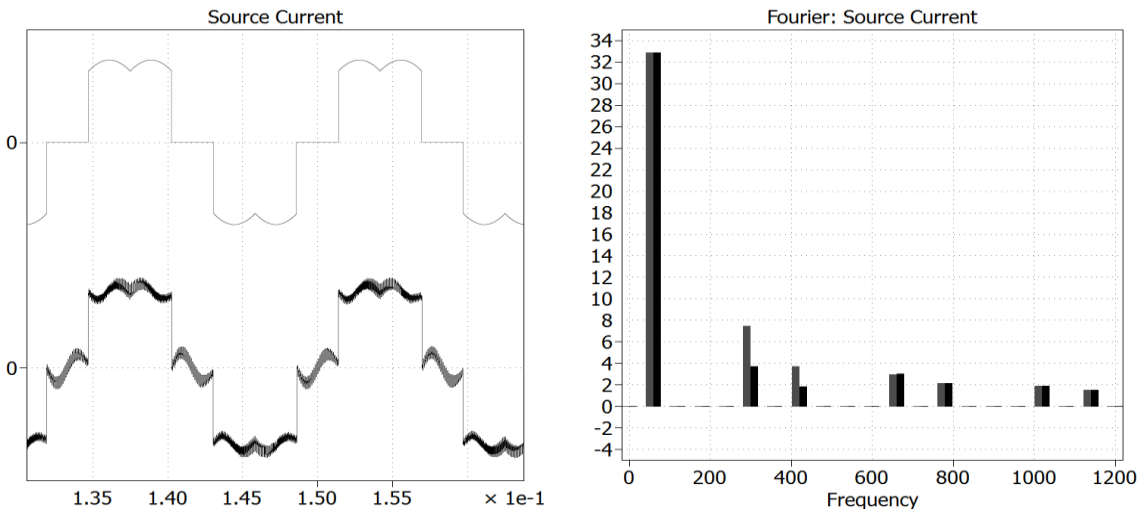

Figure 5.7: a) Source current waveform without (on top) and with active filter, b) Harmonic magnitude without (left) and with active filter

The current tracking using the PR regulator in the SRF is seen below and the results match the simulation in the previous section of a PR regulator in the stationary frame. Only one controller is required to compensate both harmonics in the SRF whereas the stationary frame needs a controller for each harmonic.

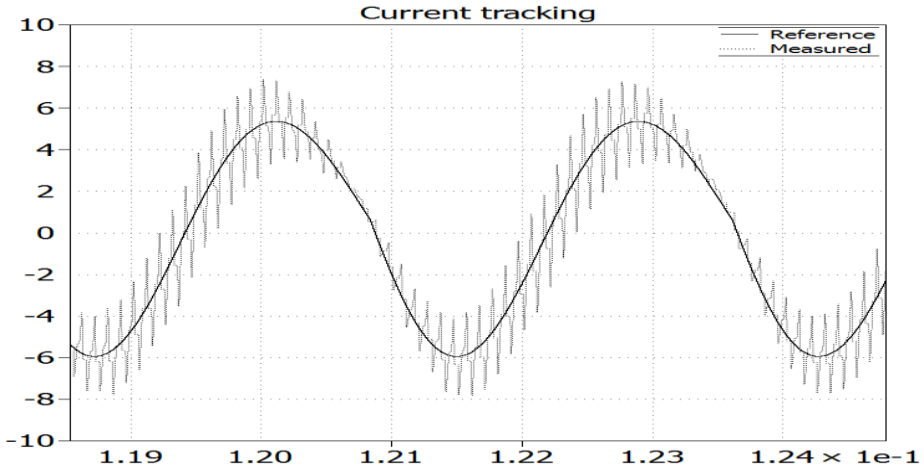

Figure 5.8: Reference current tracking using PR regulator in the synchronous frame

This method is thus effective for harmonic current compensation and since the rotating transformation is done at the fundamental frequency, a PI regulator can be used for the DC link voltage control to create a fundamental current reference that is added to the harmonic current reference. The PR regulator can effectively maintain the DC link voltage with this technique. The overview of the control diagram for this HAF is seen in Figure 5.9.

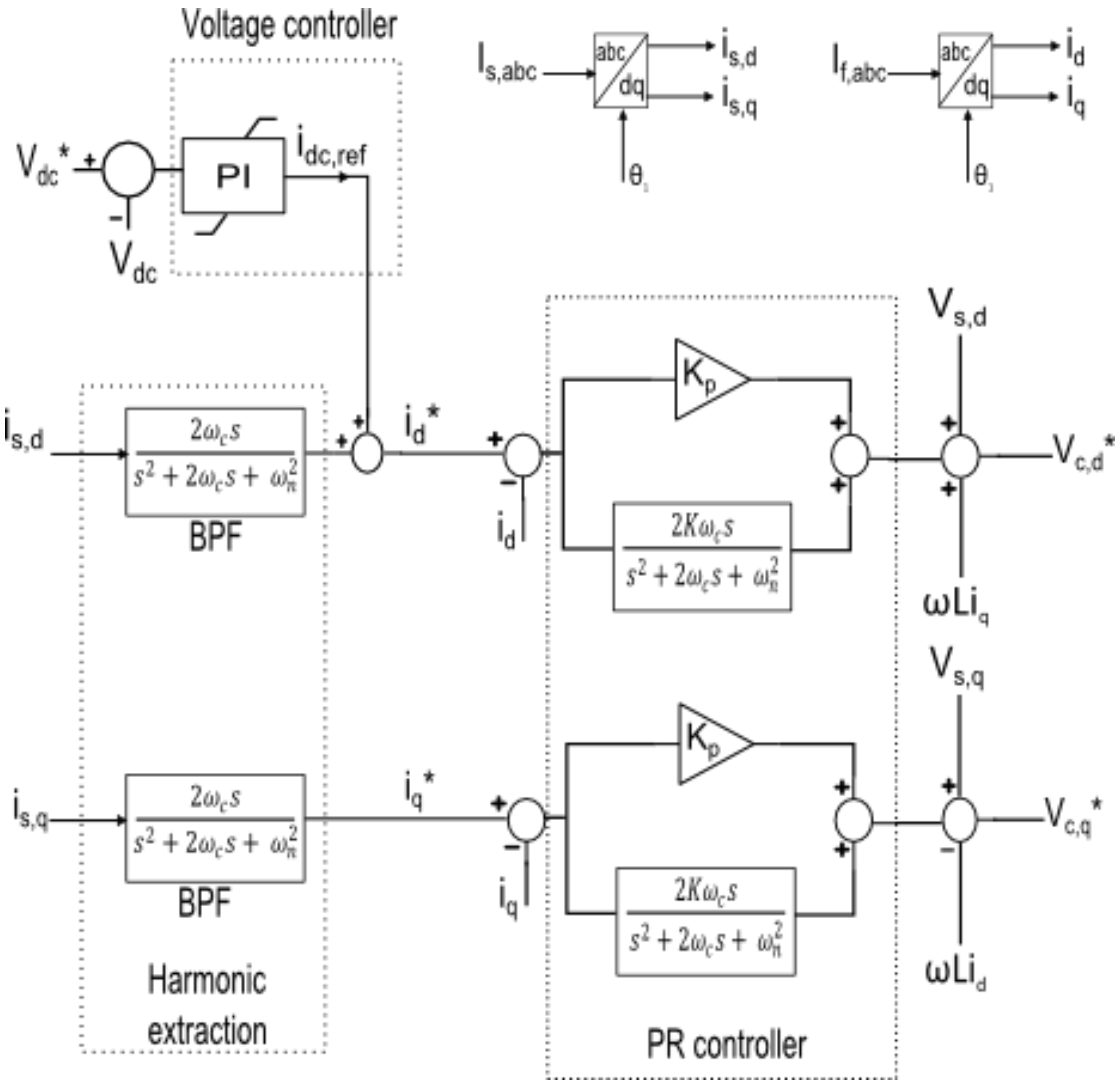

Figure 5.9: Overview of the control diagram for the active filter operation

The open loop and closed loop transfer function Bode plots for the faster current controller as well as the slower outer-loop DC voltage controller are seen in Figure 5.10 and Figure 5.11, respectively.

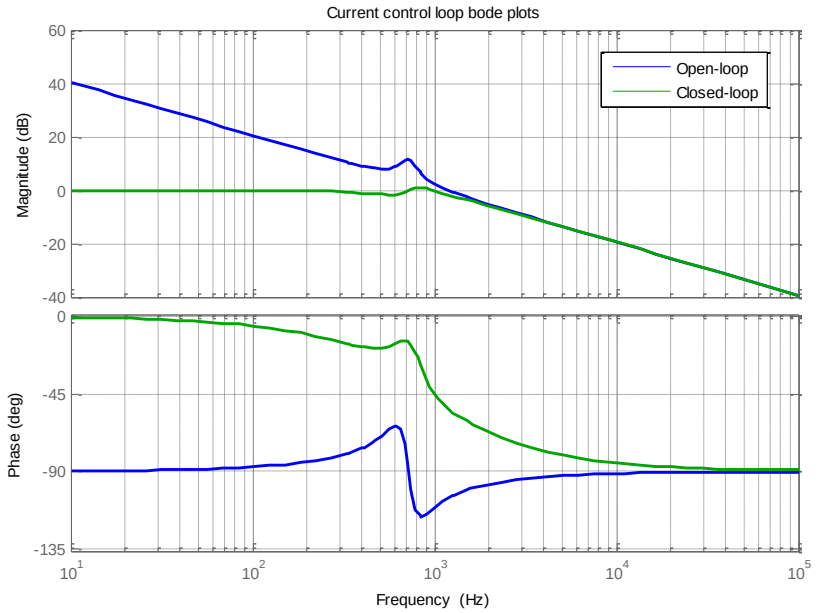

Figure 5.10: Inner current control open and closed loop transfer function Bode plot

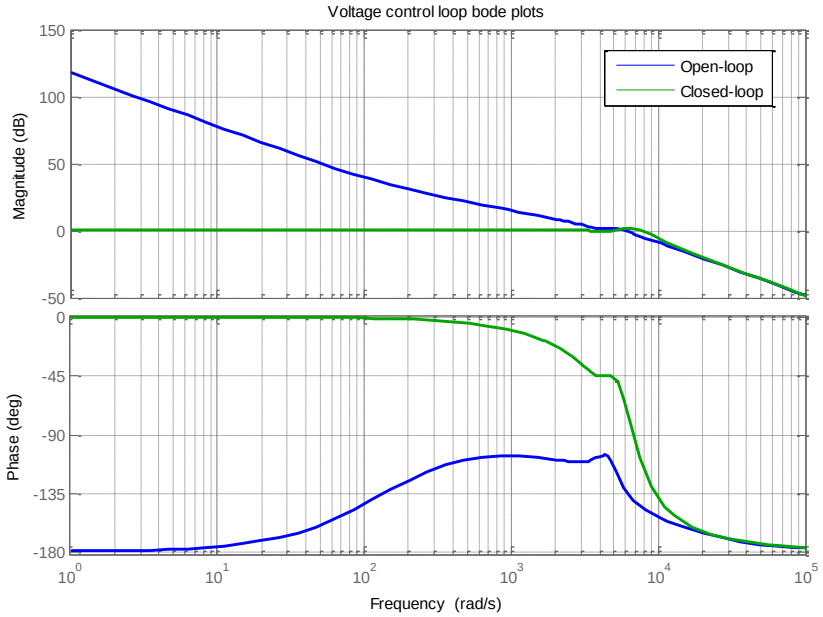

Figure 5.11: Outer voltage control open and closed loop transfer function Bode plot

5.4 Hybrid Active Filter Implementation with HVDC system

The proposed PR controller was implemented for the designed HAF HVDC system. This HAF topology was tested for the normal operating condition as well as the resonant condition that caused problems with the passive filters. During the normal condition, the active filter was not required to do harmonic compensation as the passive filter was able to sink the dominant harmonics. However, the active filter was able to divert the harmonic current during the resonant condition so that the amplified current in the grid was cancelled out. The HAF topology was able to meet the harmonic performance specifications even during the resonant condition for which the passive filters failed to meet the performance criteria in Chapter 3. The time domain simulation results are documented in Chapter 6.

CHAPTER 6

Results

The time domain simulation of the HAF connected to the HVDC system designed in Chapter 3 was done in PSCAD. The HAF performance was tested for the condition of system resonance that caused the passive filter to be ineffective as seen in the PSCAD results of Chapter 3.

6.1 PSCAD Simulation Results

In this section, the current and voltage waveforms and the derived frequency domain results for the harmonic performance metrics have been documented.

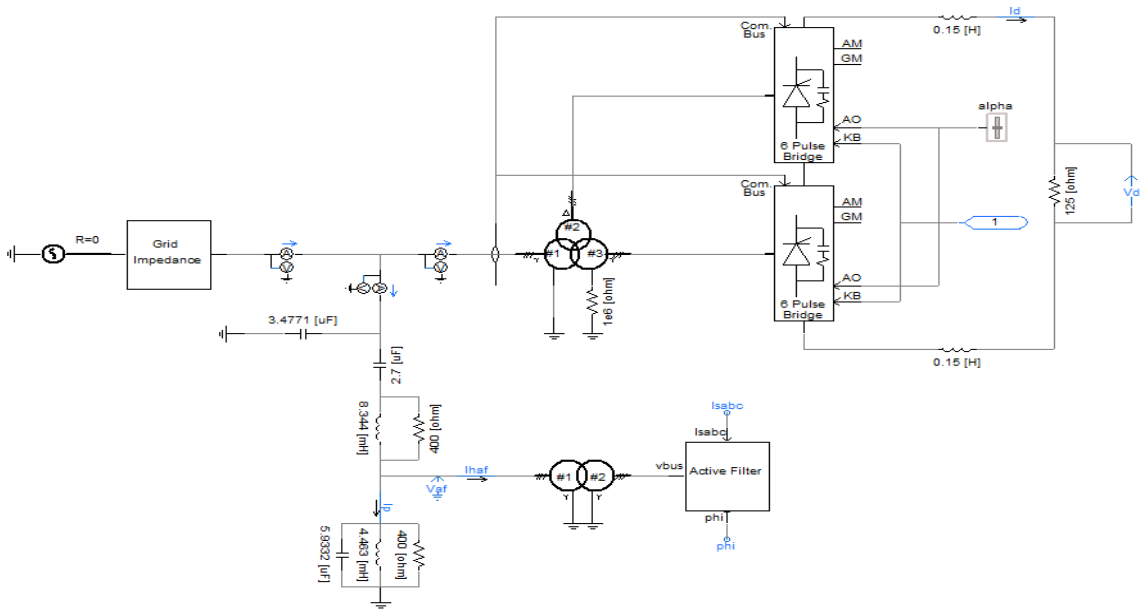

Figure 6.1: HVDC system model in PSCAD

The current waveform in Figure 6.2 shows the result of system resonance without the use of the HAF. This result is for a grid impedance value that is causing resonance at the 11th and 13th harmonics.

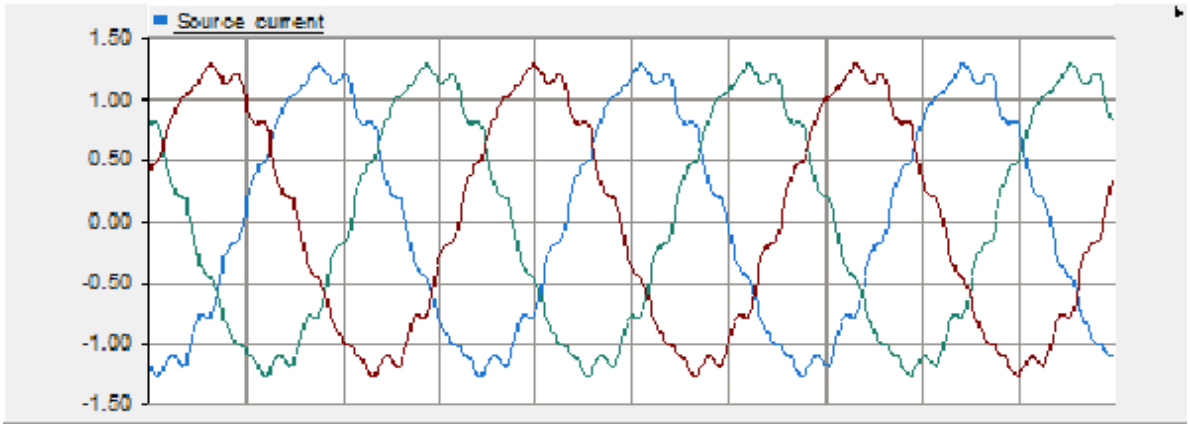

Figure 6.2: Grid current profile during system resonance without the HAF

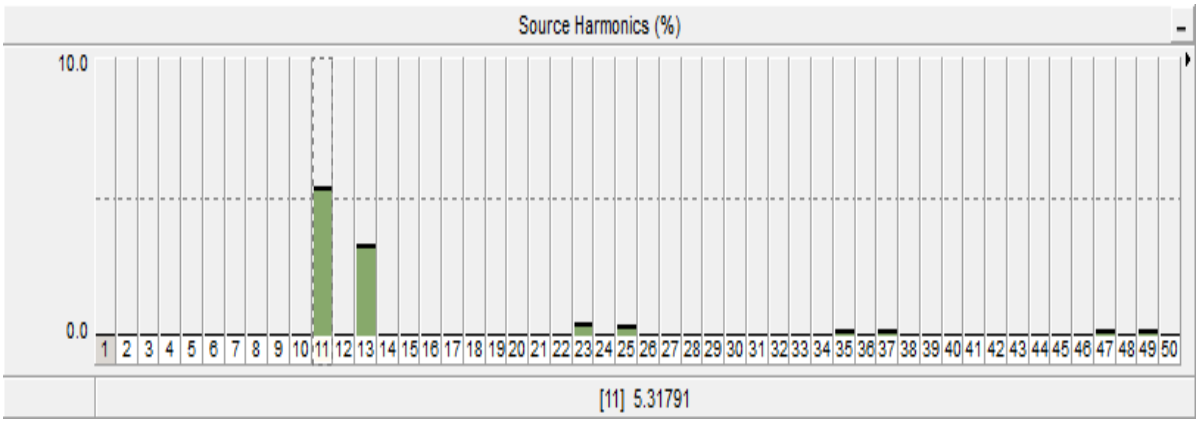

Figure 6.3: Fourier spectrum of the grid current during system resonance at dominant harmonics without the HAF

The goal of the HAF is to remove these amplified current harmonics from the source. The results that follow are with the HAF implemented during the same system resonance condition at the dominant harmonics.

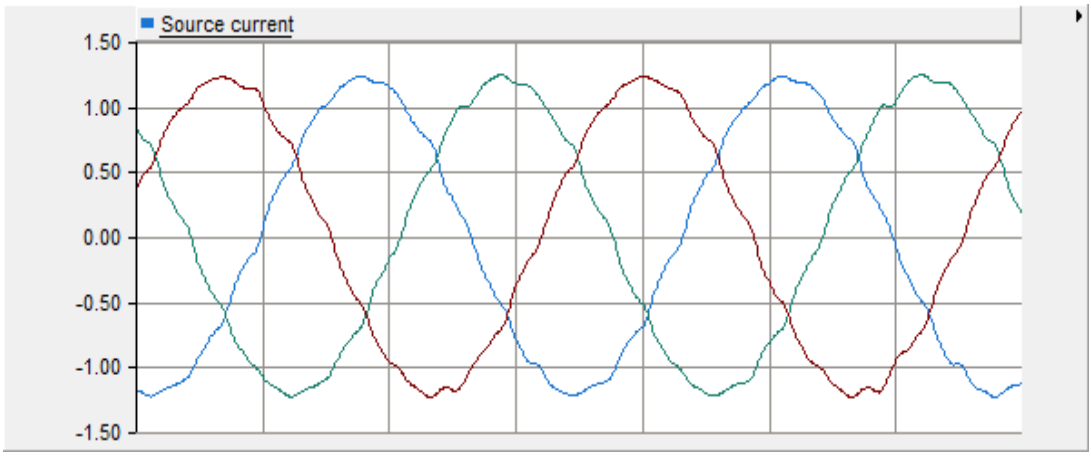

Figure 6.4: Grid current profile during system resonance with the HAF

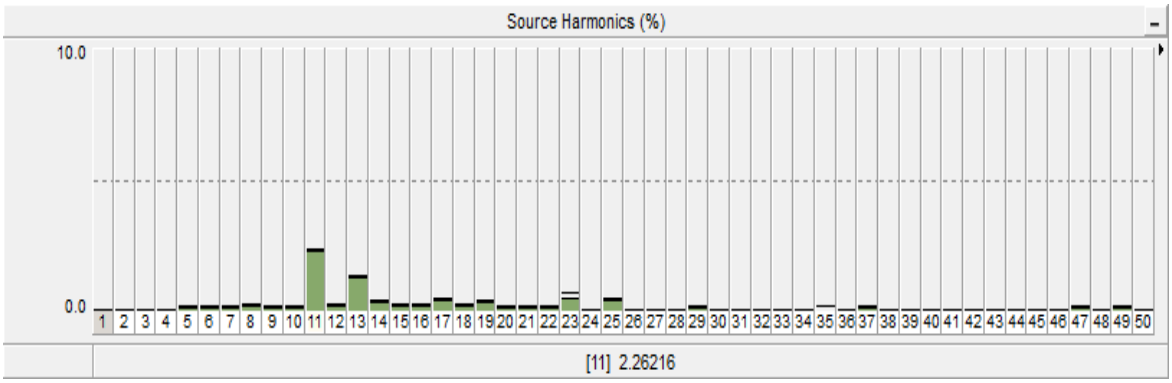

Figure 6.5: Fourier spectrum of the grid current during system resonance at dominant harmonics with the HAF

It is clear from the difference in the Fourier spectrum plot in Figure 6.3 and Figure 6.5, that the 11^{th} and 13^{th} harmonic current magnitudes are greatly reduced in the grid current due to the operation of the HAF. The load current remains unchanged and the load current waveform and Fourier spectrum plot are seen in Figure 6.6 and Figure 6.7, respectively.

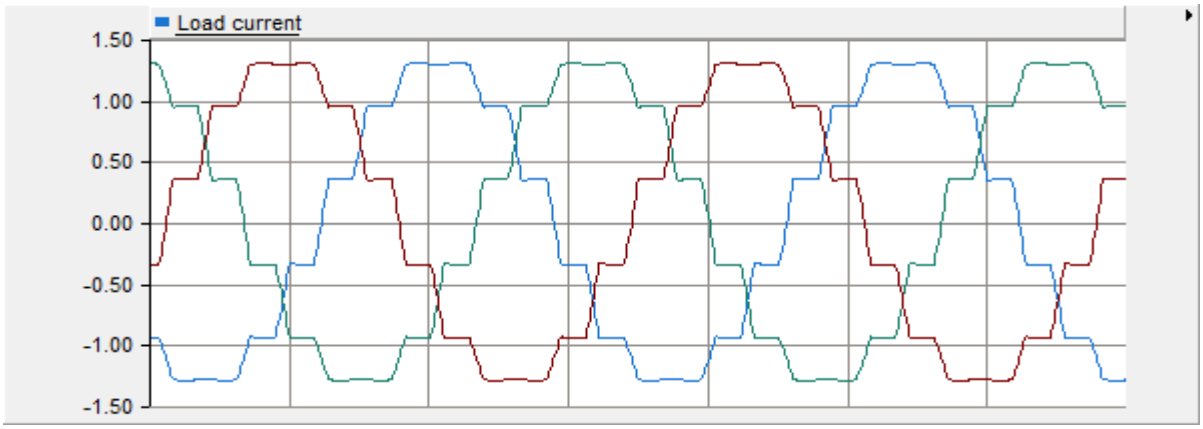

Figure 6.6: Transformer primary current waveform with HAF

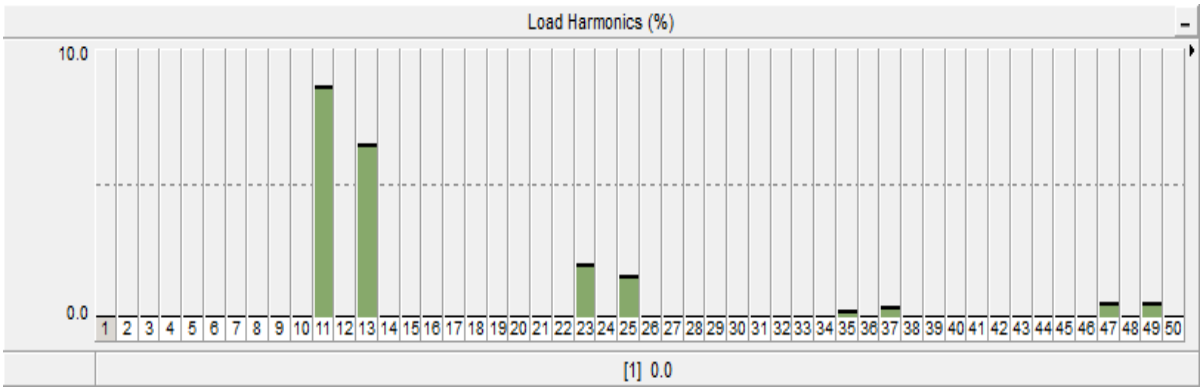

Figure 6.7: Fourier spectrum of the load current with HAF

The performance of the PR controller is seen in the tracking of the direct axis reference current by the regulator. The reference current is the sum of the DC link voltage controller as well as the harmonic reference extracted from the source. The active filter direct axis current is controlled by the PR regulator.

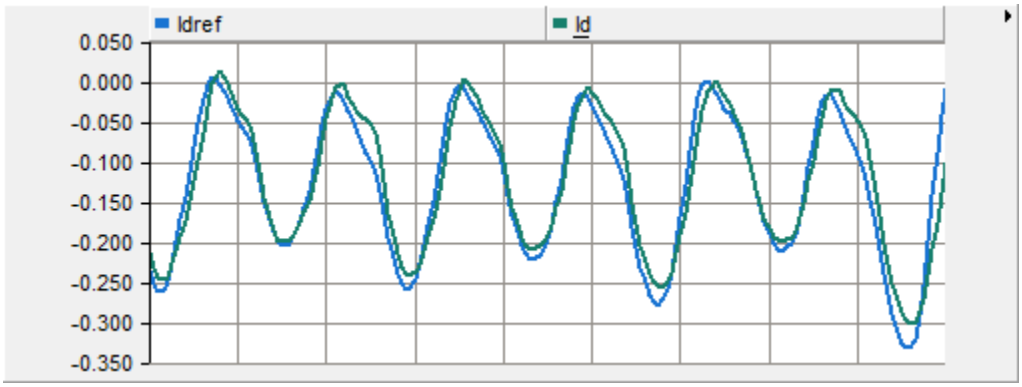

Figure 6.8: Direct axis current tracking performance of the PR regulator

The grid voltage at the PCC has very little distortion and the individual voltage distortion for all harmonics is considerable less than the 1 percent limit that is advised by the IEEE 519 Harmonic Standard.

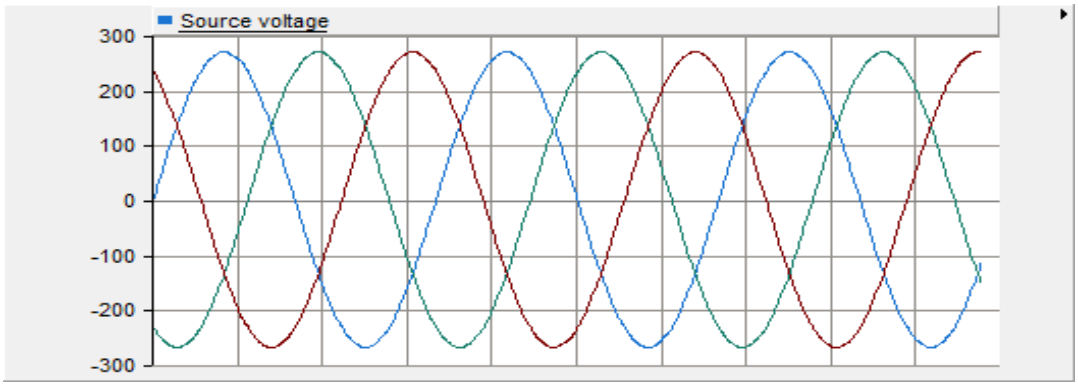

Figure 6.9: Grid voltage waveform at the PCC

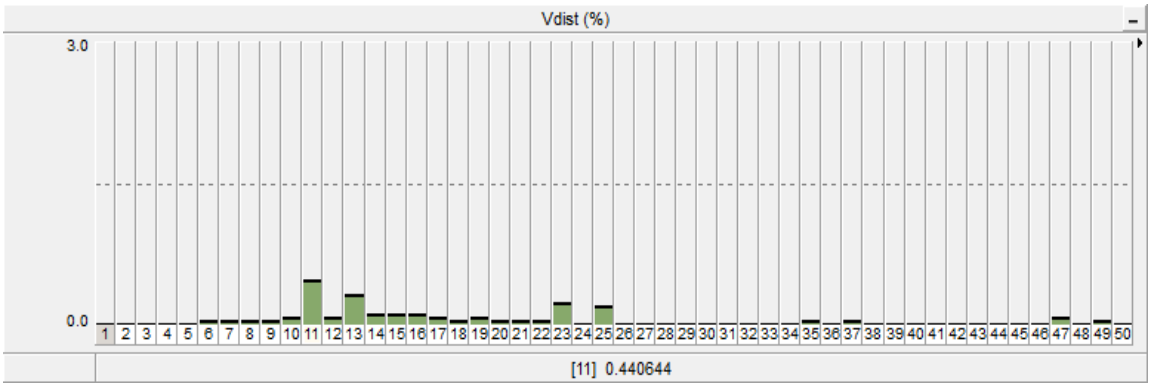

Figure 6.10: Fourier spectrum of the grid voltage at the PCC

The harmonic performance indices in the frequency domain are calculated dynamically during the simulation and are seen in the bar plots in Figure 6.11. The appropriate weighting factors and equations discussed in the harmonic standards section of chapter 2 are used for these calculations after using the Fourier transform to get harmonic information of the currents and voltages.

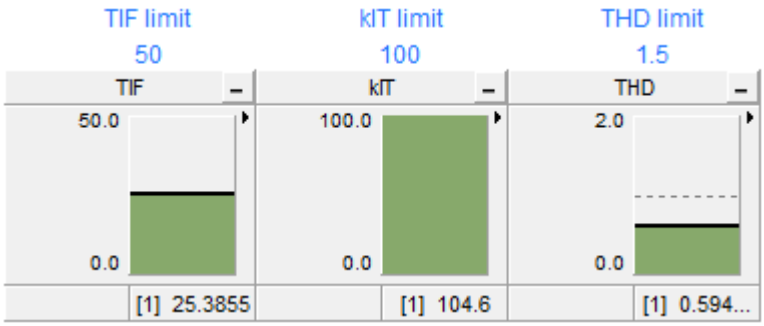

Figure 6.11: Harmonic performance indices during system resonance with the HAF

It can be seen that the performance metrics established in Chapter 2 are met with the help of the HAF even when the passive filters are debilitated due to resonance with the grid impedance.

The regulation of the DC link voltage by the PR controller is also seen below. The response time is limited by the amount of current that is allowed to go through the switches. For a 7 kV device it is normal to have a current rating of about 750 A so the saturation limit of the control is set to 700 A [25].

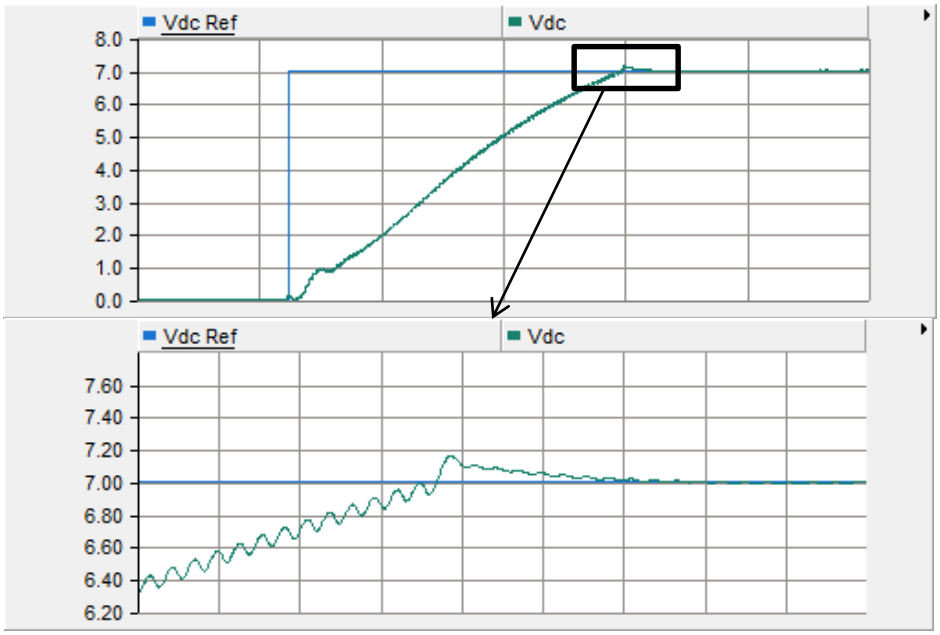

Figure 6.12: DC link voltage step response

The overshoot is controlled by having a high damping factor to get a high phase margin. The DC link voltage tracking during harmonic compensation is seen in Figure 6.13.

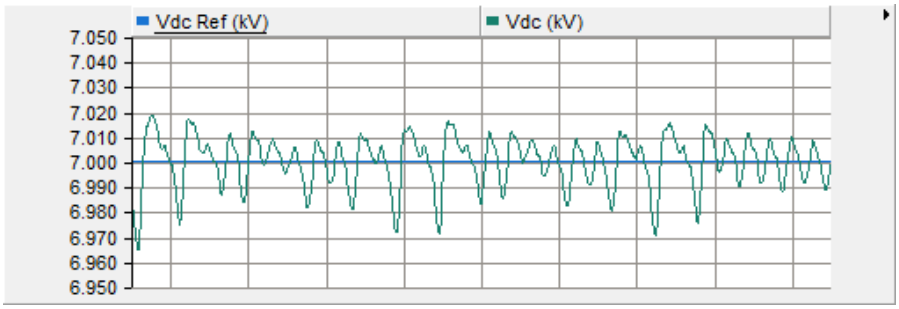

Figure 6.13: DC link voltage tracking during harmonic current compensation

The active filter rating is found to be less than 1% of the HVDC converter rating of 500 MW. As can be seen by the plot in Fig. 6.14, the active filter has a rating of less than 0.4 MVA during the worst case harmonic current compensation.

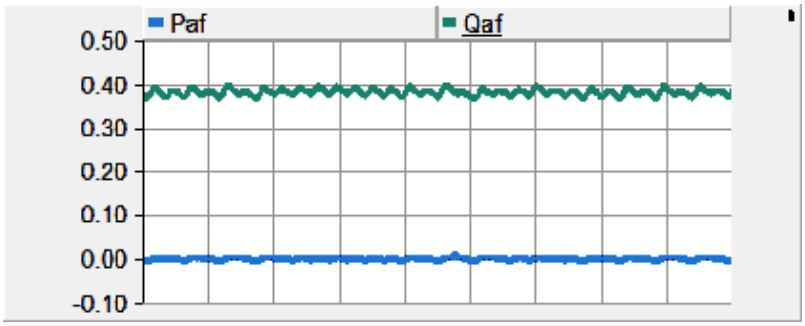

Figure 6.14: Active filter power during harmonic current compensation

For a condition where there is no system resonance and the passive filters are able to remove the harmonic currents, the rating of the active filter is reduced to a little more than 0.1% of the HVDC converter rating.

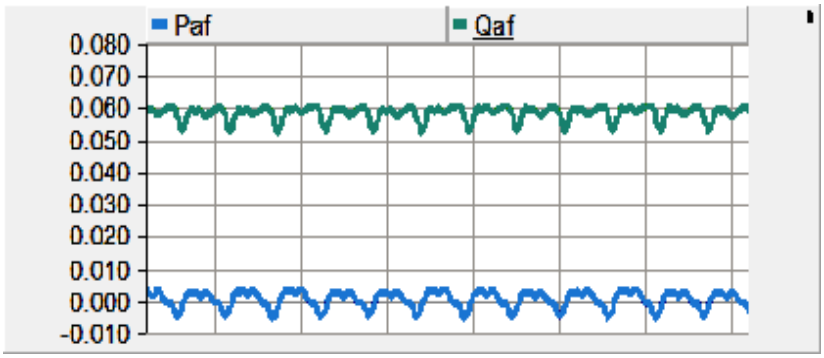

Figure 6.15: Active filter power during optimal passive filtering

6.2 RTDS Simulation Results

The entire HVDC system was also simulated in RTDS to confirm the PSCAD results. However, an average model of the VSC was used instead of the complete switching model due to limitations of the maximum switching frequency in RTDS.

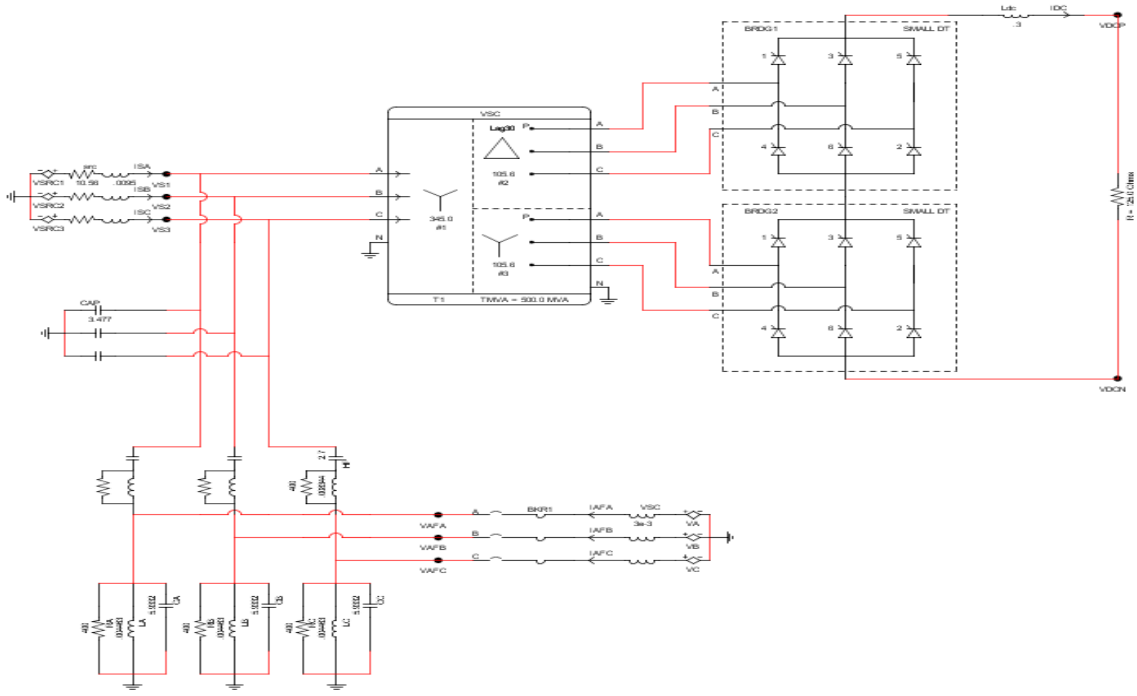

Figure 6.16: HVDC system model in RTDS

The following results are obtained from the simulation of the small time step model seen in Fig. 14. The LCC output DC voltage and DC current are recorded in Figure 6.17 during the normal operating condition to verify the HVDC converter output requirements are met.

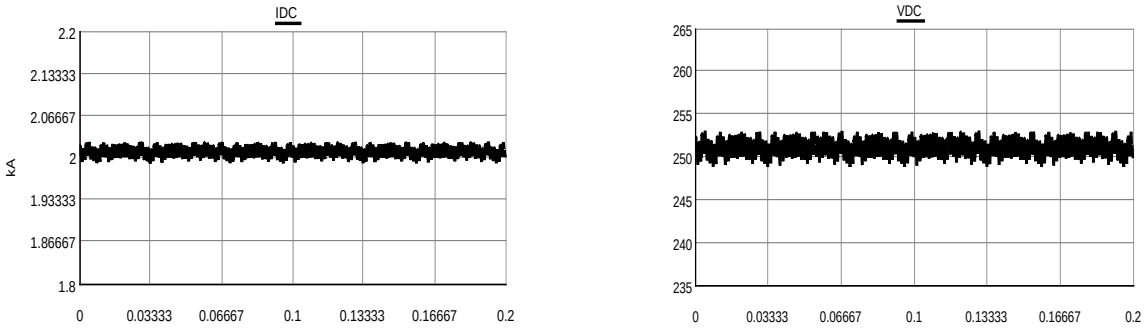

Figure 6.17: HVDC converter output - a) DC current, b) DC Voltage

The results of the grid current and voltage without and then with the passive filters is seen in Figure 6.18 and Figure 6.19, respectively.

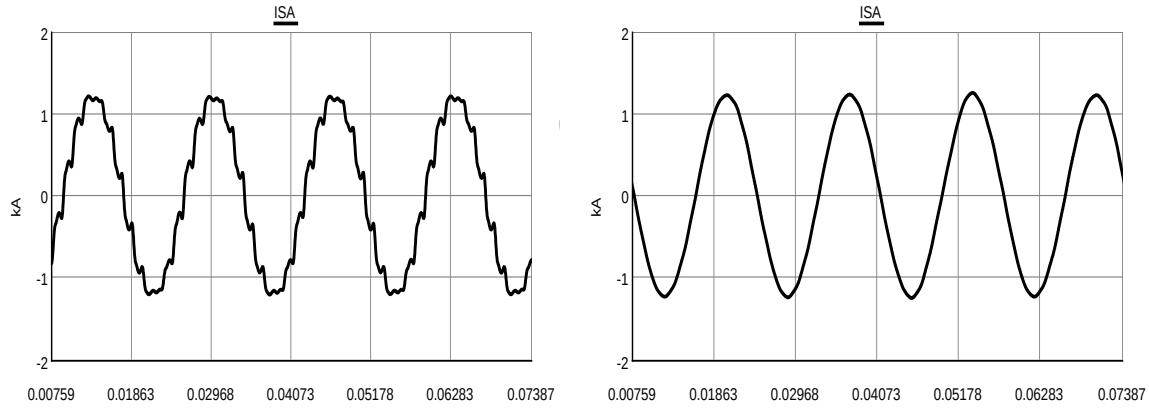

Figure 6.18: Grid current without passive filters (left) and with passive filters (right)

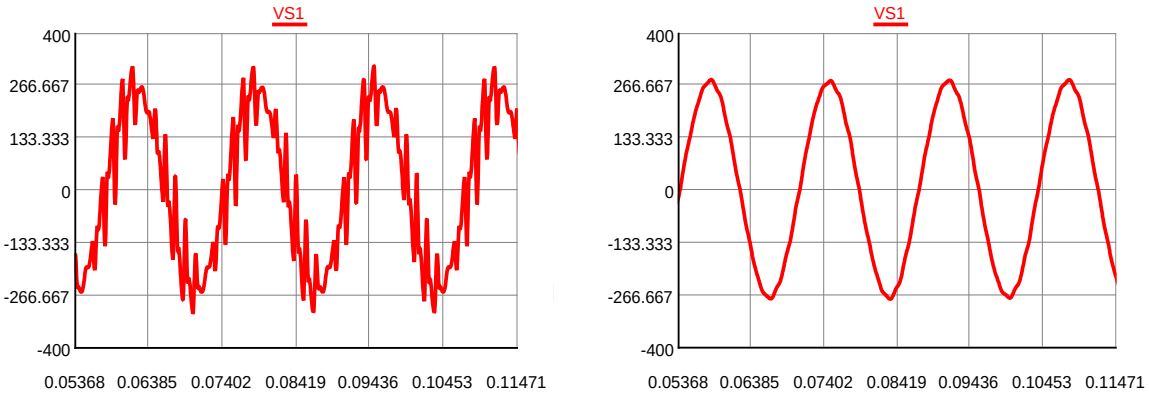

Figure 6.19: Grid voltage without passive filters (left) and with passive filters (right)

The system resonance condition was then investigated by changing the impedance of the AC grid to cause resonance with the passive filters at the dominant harmonics. The waveform of the source current during this condition is seen in Figure 6.20.

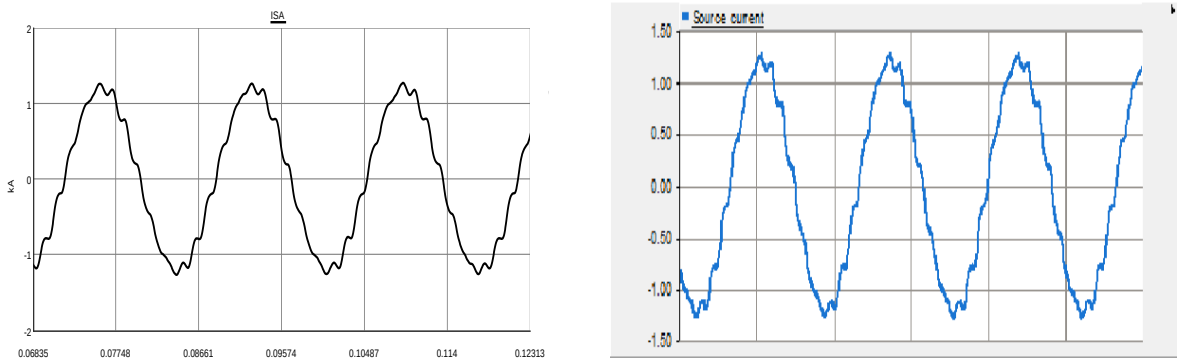

Figure 6.20: Grid current profile during system resonance without the HAF in RTDS (left) and PSCAD (right)

And the grid current waveform with the application of the HAF average model is seen to improve due to the compensation of the harmonic currents by the active filter.

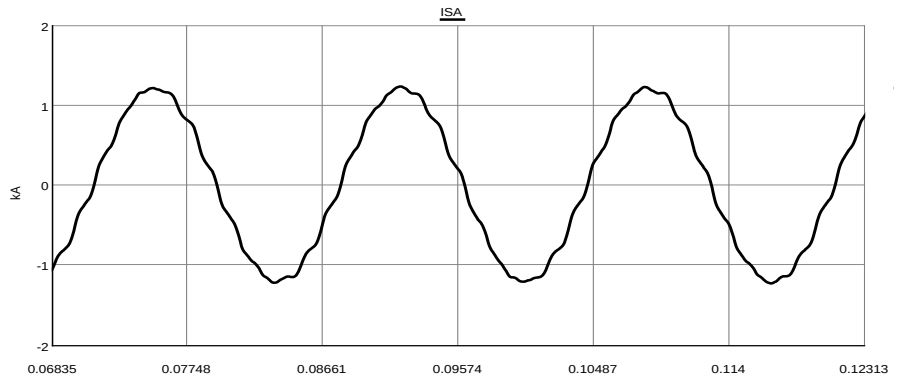

Figure 6.21: Grid current profile during system resonance with the HAF

The performance of the HAF directly after being turned on for harmonic current compensation is seen in Figure 6.22.

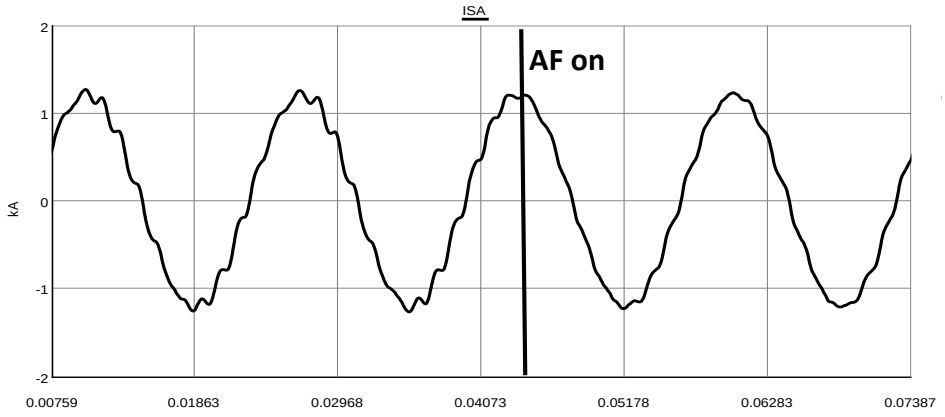

Figure 6.22: Grid current before and after turning on Active Filter

CHAPTER 7

Summary and Future Work

A unique topology for a hybrid active filter is implemented and its performance for harmonic current filtering is verified through time domain simulations. The HAF strategy is useful to overcome the shortcomings of passive filters and at the same time lower the rating of the active filter. The HAF is able to provide filtering support when current amplification occurs at the dominant harmonic frequencies due to the resonance between the grid and the filter impedances. It was shown in the simulation that the HAF is able to meet the harmonic performance specifications outlined by the IEEE 519 standard for distortion and other commonly accepted telephone interference guidelines.

An important step in further improvement of the suggested HAF is to conduct a detailed study of the power transfer from the active filter to help reduce the rating of the converter. Due to the presence of harmonic voltage and current at the active filter, an understanding of the harmonic power transfer is crucial for the appropriate tuning of the passive components and reduction in the size of the converter. Further, the optimization of the control parameters and the transformer leakage reactance will contribute to a smaller dc bus requirement and reduce the rating of the IGBTs of the converter. The turns ratio can be used to reduce the voltage seen by the active filter but this results in a higher converter side current requirement for matching the reference value. Due to the line reactance, the voltage

drop across the inductor is higher for a larger current which results in a larger DC link voltage requirement.

Once the system is optimized, the active filter can be modeled in the Typhoon Hardware-in-the-Loop (HIL) and an external power electronics controller can be used to create the switching pulses for the real-time emulation of the power converter. The Typhoon HIL can then be interfaced with the rest of the system that is already modeled in the RTDS. This is an industry standard method of power system emulation using HIL. Finally, the HAF should be implemented in hardware to test the results of the simulation and to confirm its application for harmonic filtering of practical systems.

REFERENCES

[1] W. Hammer, "Dynamic Modeling of Line and Capacitor Commutated Converters for HVDC Power Transmission," *Swiss Federal Institute of Technology*, Zurich, SUI, 2003.

[2] N. Mohan, C. Wong, "Active Filters for High-Voltage-Direct-Current (HVDC) Converter Terminals," *Prepared by University of Minnesota, Electric Power Research Institute*, 1988.

[3] G. D. Breur, J. H. Chow, T. J. Gentile, C. B. Lindh, G. Addis, R. H. Lasseter, J. J. Vitharyathil, "HVDC-AC System Interaction from AC Harmonics," *Prepared by General Electric Company, Electric Power Research Institute*, 1982.

[4] M. I. Hussain, "Aspects of Design of Harmonic Filters for HVDC System," *The University of New Brunswick*, CAN, 1972.

[5] "High-Voltage Direct Current (HVDC) Systems – Guidebook to the Specification and Design Evaluation of a.c. Filters," *Bureau of Indian Standards*, New Delhi, IND, 2013.

[6] C. K. Duffey, R. P. Stratford, "Update of Harmonic Standard IEEE-519 IEEE Recommended Practices for Harmonic Control in Electric Power Systems," *Power Technologies, Inc.*, Schenectady, NY, 1988.

[7] N. G. Hingorani, M. F. Burbery, "Simulation of AC System Impedance in HVDC System Studies," *IEEE Transactions on Power Apparatus and Systems*, vol. PAS-89, no. 5, pp. 820, 828, 1970.

[8] M. D. Heffernan, “Analysis of AC/DC System Disturbances,” *University of Canterbury*, NZL, 1980.

[9] D. A. Woodford, “HVDC Transmission,” *Manitoba HVDC Research Centre*, CAN, 1998.

[10] M. A. Zamani, M. Mohseni, “Damped-Type Double Tuned Filters Design for HVDC Systems,” *Electrical Power Quality and Utilisation*, 2007.

[11] X. Yao, “Algorithm for the parameters of double tuned filter,” *Harmonics and Quality of Power Proceedings*, 1998.

[12] T. M. Haileselassie, “Control of Multi-terminal VSC-HVDC Systems,” *Norwegian University of Science and Technology*, NOR, 2008.

[13] T. Kalitjuka, “Control of Voltage Source Converters for Power System Applications,” *Norwegian University of Science and Technology*, NOR, 2011.

[14] S. Sul, “Control of Electric Machine Drive Systems,” *Wiley-IEEE Press*, 2011.

[15] H. El Brouji, P. Poure, S. Saadate, “Study and comparison of fault tolerant shunt three-phase active filter topologies,” *Power Electronics and Motion Control Conference*, 2006.

[16] A. L. Plaisant, “Active Filtering of AC Harmonics from HVDC Converters,” *University of Waterloo*, CAN, 1997.

[17] A. van Zyl, J. H. R. Enslin, W. H. Steyn, R. Spree, “A New Unified Approach to Power Quality Management*,” Power Electronics Specialists Conference*, 1995.

[18] C. Wong, N. Mohan, S. E. Wright, K. N. Mortensen, "Feasibility study of AC- and DC- side active filters for HVDC converter terminals," *Power Delivery, IEEE Transactions on,* vol. 4, no.4, pp.2067,2075, 1989.

[19] F. Z. Peng, H. Akagi, A. Nabae, "Compensation characteristics of the combined system of shunt passive and series active filters," *Industry Applications, IEEE Transactions on,* vol. 29, no. 1, pp. 144,152, 1993.

[20] S. T. Senini, P. Wolfs, "Systematic identification and review of hybrid active filter topologies," *Power Electronics Specialists Conference,* 2002.

[21] P. Cheng, "Use of Dominant Harmonic Active Filters in High Power Applications*," University of Wisconsin – Madison,* 1999.

[22] M. Rastogi, N. Mohan, A. Edris, "Filtering of harmonics currents and damping of resonances in power systems with a hybrid-active filter," *Applied Power Electronics Conference and Exposition,* 1995.

[23] P. Cheng, S. Bhattacharya, D. M. Divan, "Hybrid solutions for improving passive filter performance in high power applications*," Applied Power Electronics Conference and Exposition,* 1996.

[24] D. N. Zmood, D. G. Holmes, "Stationary frame current regulation of PWM inverters with zero steady-state error," *Power Electronics Specialists Conference*, 1999.

[25] Infineon, "6.5 kV IGBT modules," *FZ750R65KE3 datasheet,* Rev. 3.0, Jun. 2014.

[26] "IEEE Recommended Practices and Requirements for Harmonic Control in Power Systems," *IEEE Standards Board*, New York, NY, 1993.

[27] R. H. Park, "Abridgment of two-reaction theory of synchronous machines generalized method of analysis – Part I," *A.I.E.E., Journal of the*, vol. 48, pp. 194,194, 1929.

[28] L. Herman, B. Blazic, I. Papic, "Performance of a Parallel Hybrid Active Filter with Selective Harmonic Control*," Power and Energy Society General Meeting (PES)*, 2013 IEEE, vol., no., pp. 1,5,21-25, 2013.

[29] J. Arrillaga, N. R. Watson, "Power System Harmonics," *John Wiley & Sons, Inc.*, New York, NY, 2001.

APPENDICES

Appendix A

Synchronous Reference Frame

The basis of the rotating reference frame transformation and the chosen convention for this transformation is discussed in this section of the appendix. The dq0 transformation rotates the reference frame of three-phase systems to simplify the analysis of three-phase circuits. For balanced three-phase circuits, the dq0 transform reduces the three-phase AC quantities to two DC components that are defined on the direct and quadrature axis. The transformation was originally proposed by R. H. Park in [27].

The transformation and inverse transformation matrices are given below –

$$P = \frac{2}{3}\begin{bmatrix} \cos(\theta) & \cos\left(\theta - \frac{2\pi}{3}\right) & \cos\left(\theta + \frac{2\pi}{3}\right) \\ \sin(\theta) & \sin\left(\theta - \frac{2\pi}{3}\right) & \sin\left(\theta + \frac{2\pi}{3}\right) \\ \frac{1}{2} & \frac{1}{2} & \frac{1}{2} \end{bmatrix} \quad so\ that\ \ V_{dq0} = PV_{abc}$$

$$P^{-1} = \begin{bmatrix} \cos(\theta) & \sin(\theta) & 1 \\ \cos\left(\theta - \frac{2\pi}{3}\right) & \sin\left(\theta - \frac{2\pi}{3}\right) & 1 \\ \cos\left(\theta + \frac{2\pi}{3}\right) & \sin\left(\theta + \frac{2\pi}{3}\right) & 1 \end{bmatrix} \qquad so\ that\ V_{abc} = P^{-1}V_{dq0}$$

The transformation angle theta is chosen so that

$$V_d = V_m \quad and \quad V_q = 0$$

$$where\ V_m\ is\ the\ amplitude\ of\ the\ 3\phi\ signal$$

Appendix B

PLECS Simulation Results

The entire HVDC system was also designed in PLECS as a confirmation of the PSCAD simulation results.

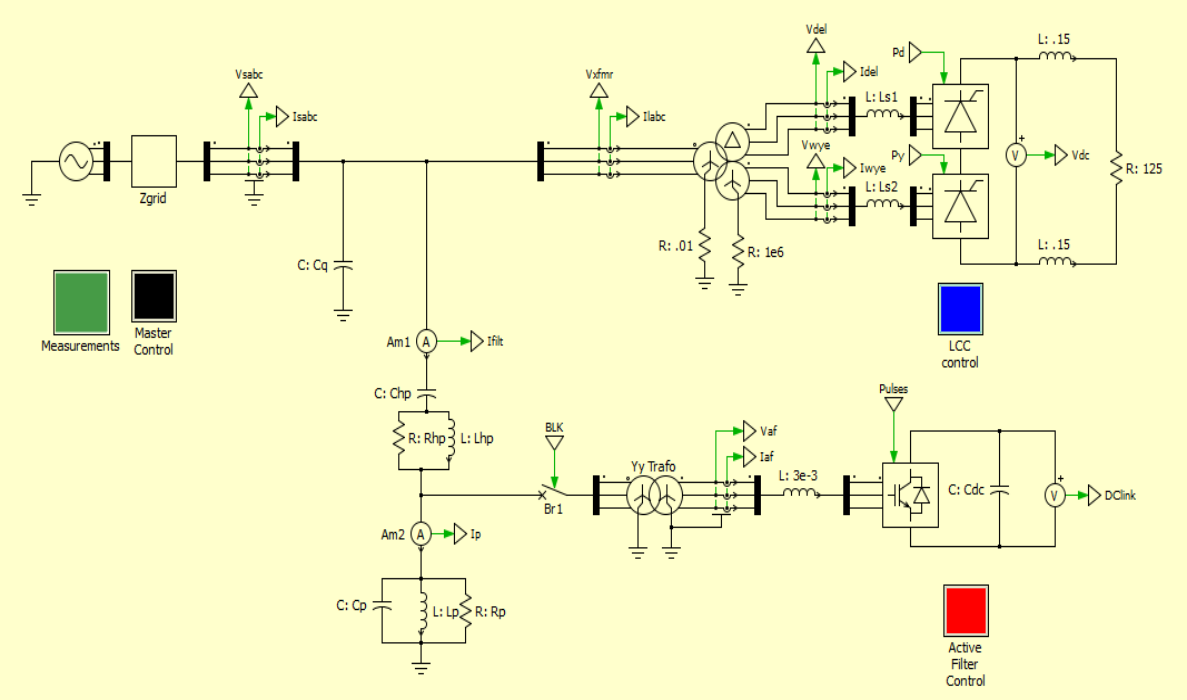

Figure: HVDC system model in PLECS

The important results of the HAF performance during the resonant condition are documented in this appendix.

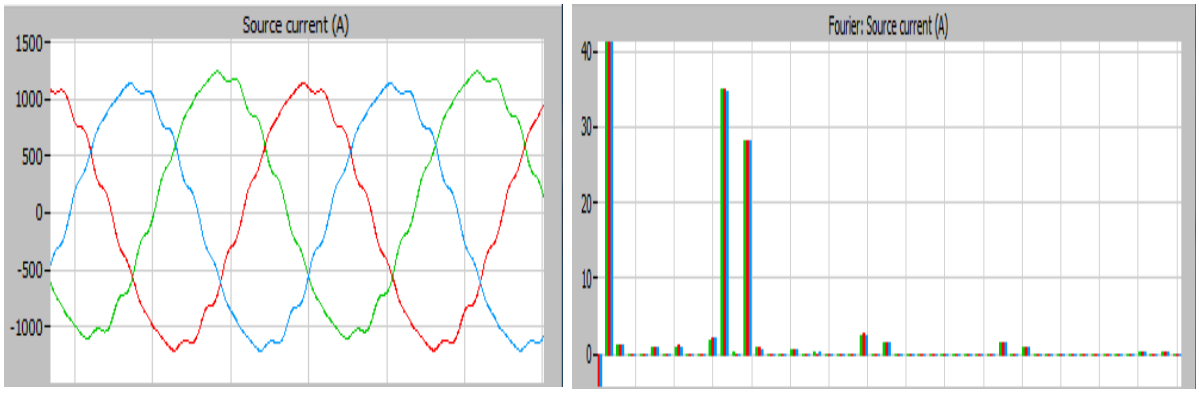

Figure: Grid current during system resonance without the HAF

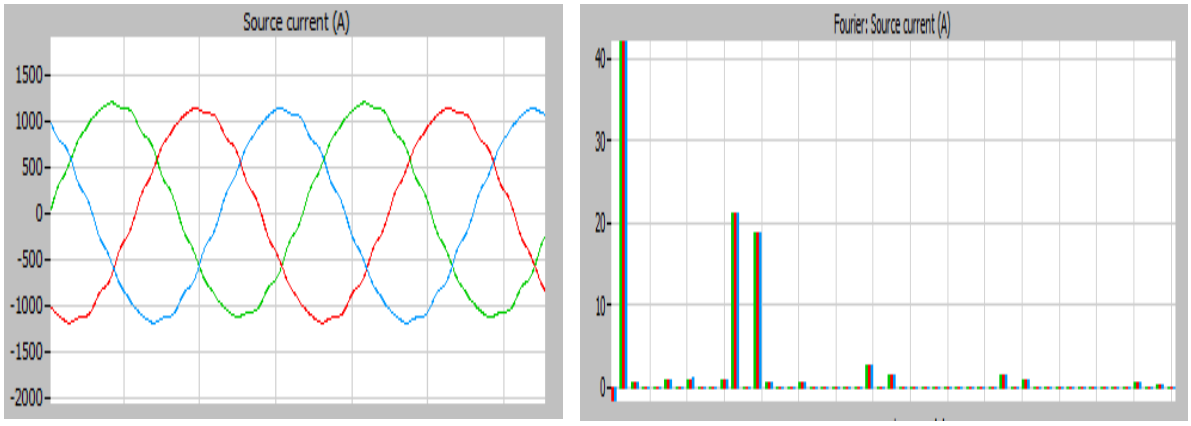

Figure: Grid current during system resonance with the HAF

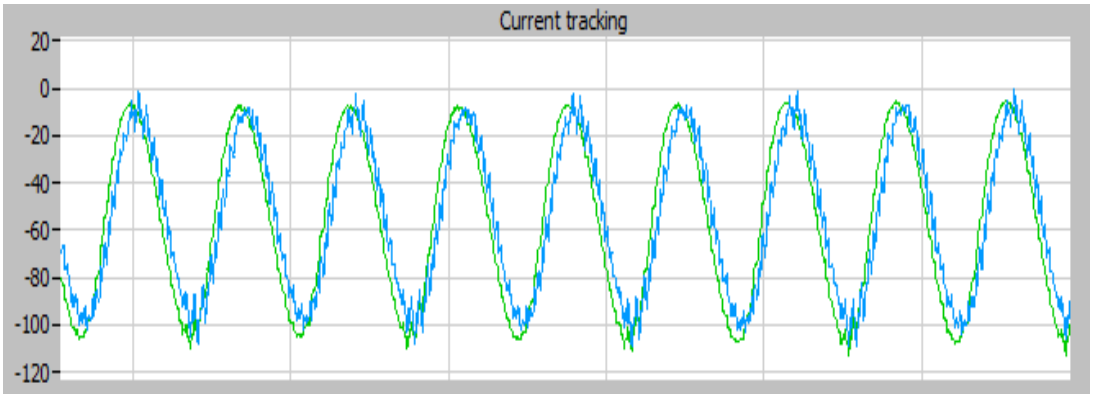

Figure: Reference current tracking performance of the PR controller

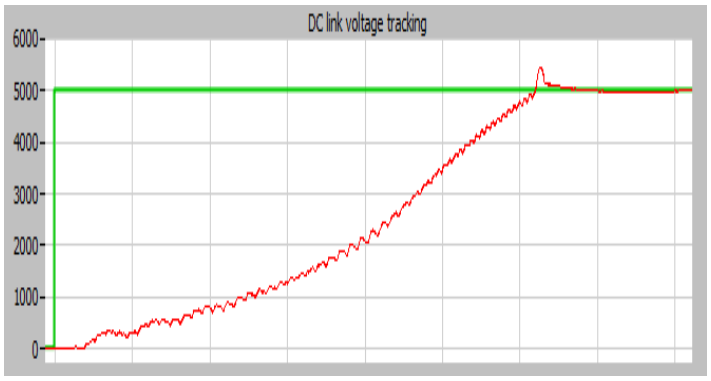

Figure: DC link voltage step response

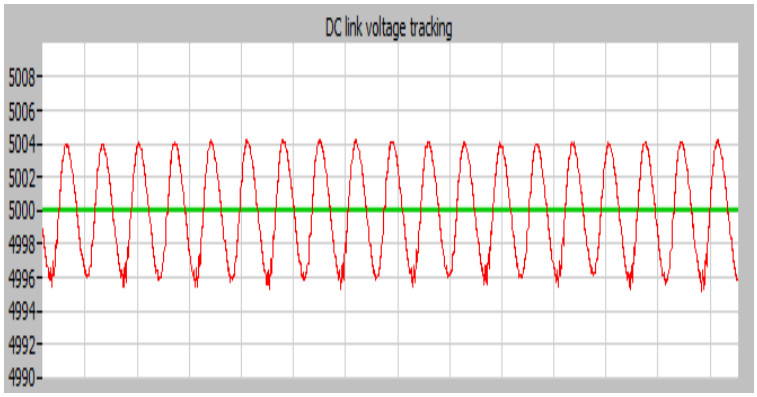

Figure: DC link voltage control during harmonic current compensation